Annual Reports C
Dynamic Article Links

Cite this: *Annu. Rep. Prog. Chem., Sect. C*, 2011, **107**, 14–46

www.rsc.org/annrepc
REVIEW

Partly-quenched systems containing charges. Structure and dynamics of ions in nanoporous materials

Barbara Hribar-Lee, Miha Lukšič and Vojko Vlachy*

DOI: 10.1039/c1pc90001c

Disordered porous materials filled with liquid or solution may be considered as partly-quenched, *i.e.*, as systems in which some of the degrees of freedom are quenched and others annealed. In such cases, the statistical-mechanical averages used to calculate the system's thermodynamical properties become double ensemble averages: first over the annealed degrees of freedom and then over all possible values of the quenched variables. In this respect, the quenched-annealed systems differ from regular mixtures. The multi-faceted applications of the partly-quenched systems to a kaleidoscope of technological and biological processes make the understanding of these systems important and of interest. Present contribution reviews recent developments in theory and simulation of partly-quenched systems containing charges. Specifically, two different models of such systems are discussed: (a) the model in which the nanoporous system (matrix subsystem) formed by charged obstacles is electroneutral, and (b) the model, where the subsystem of obstacles has some net charge. The latter model resembles, for example, the situation in ion exchange resins *etc.* Various theoretical methods are applied to investigate structural and dynamical peculiarities of such systems. One is the replica Ornstein-Zernike theory, especially adapted for charged systems, and the other is the Monte Carlo computer simulation method. These two approaches are well suited to study thermodynamical parameters, such as the mean activity coefficient of the annealed electrolyte or Donnan's exclusion parameter. Highly relevant issue of dynamics of ions in partly-quenched systems is also addressed. For this purpose, the Brownian dynamic method is used: the self-diffusion coefficients of ions are calculated for various model parameters and discussed in light of the experimental data. These results, together with the thermodynamical data mentioned above, provide additional evidence that properties of the adsorbed fluid substantially differ from those of its bulk counterpart.

University of Ljubljana, Faculty of Chemistry and Chemical Technology, Aškerčeva c. 5, SI-1000 Ljubljana, Slovenia. E-mail: vojko.vlachy@fkkt.uni-lj.si

Highlights

In the present review article, we highlight the major advancements in theory and simulation of partly-quenched systems containing charges. One of the most important steps was the development of the integral equation theory for such systems. The replica Ornstein-Zernike equation theory in the hypernetted-chain approximation yields results in good agreement with computer simulations. In combination with the formula for the excess chemical potential, the theory represents an excellent tool to study electrolyte adsorption in charged matrices. Notice that replica theory requires only the pair distribution function (or the structure factor) of obstacles as an input for the calculation. In the last years, the studies of thermodynamical properties of nanoporous adsorbents were complemented by examination of dynamics of ions and molecules of the annealed phase. This approach, together with more realistic modelling of the porous material based on the experimental data, shall yield further progress in understanding these systems.

1. Introduction

Understanding thermodynamical and structural properties of systems where the mobility of at least one component is considerably smaller than the mobilities of the others (for example, high molecular polyelectrolytes and colloidal dispersions) is of importance for basic research, as well as for technology. In the extreme case where the mobility of one component is zero and the other components can move freely, we have the so-called partly-quenched system. Continuum systems with quenched disorder, such as nanoporous materials, gels, amorphous substances, clays, engineering composites *etc*., are of interest for medicine, separation science, and catalysis, as well as for various technologies.

The progress in statistical-mechanical theories of continuum systems with quenched disorder made before the year 2000 was reviewed by Pizio, Sokołowski, and Rosinberg.[1–3] The pioneering contributions to this area of research are due to Madden and Glandt, Given and Stell, Rosinberg, Bratko and Chakraborty, Chandler, Tosi, Pizio, Lomba, and others.[4–28] The theoretical research was stimulated by observations indicating that properties of an adsorbed fluid differ in several aspects from those of the unperturbed bulk fluid.[29–33]

The great majority of the above-mentioned studies was concerned with systems characterised by short-range interactions, such as hard spheres or Lennard-Jones fluids. The partly-quenched systems containing charges have received less attention and have not been thoroughly reviewed so far. This is in discrepancy with their scientific, medicinal and industrial importance. The review presented here is intended to fill this gap.

This paper is organised more or less in a chronological order, emphasising the contributions for which the authors believe that they are important. This makes the article, as every other review paper, a bit subjective. It is therefore possible that some of the works related to the discussed field of research will not received adequate attention or that they were not known to the authors at the time of the writing. The contributions to this area of research are namely spread through the engineering, physico-chemical, as also purely physical journals, what makes it rather difficult to follow the progress.

After the present introductory part and the necessary overview of the basics of the theory and simulation of partly-quenched systems, the analysis will be organised in sub-chapters based on a particular group of papers. Some of the key papers are briefly introduced below.

We will start the review with the paper of Bratko and Chakraborty.[27] We found the above-mentioned study to be one of the most important early contributions concerned with the partly-quenched systems containing charges. The authors utilised the Monte Carlo simulation to show very clearly an influence of the so-called pre-quenching conditions on the adsorption in such systems. Consider a ‘‘mixture’’ consisting of two (electroneutral) ionic fluids: one quenched and one annealed. In contrast to the regular mixture, where both component are fully annealed and only one temperature (temperature of observation) applies, the major distinction for partly-quenched system is that the obstacles can be prepared under different conditions (temperature, dielectric constant) than it is the condition at which the full system is examined. This yields very interesting phenomena related to the fact that the invading electrolyte can be, depending on the spatial distribution of charged obstacles, either over- or under-screened.[27]

Bratko and Chakraborty's paper[27] and some other works published at that time had prompted Pizio and coworkers[34–37] to initiate the integral-equation study based on the replica Ornstein-Zernike equation. There is a clear distinction between the thermodynamical systems with short-range potentials, such as Lennard-Jones or similar, and Coulomb systems when treated *via* the integral equation approach. It is known from studies of the bulk ionic fluids (see, for example, ref. 38) that the pair-potential needs to be ‘‘re-normalised’’, *i.e.*, the short-range and the long-range (Coulomb) part of the pair-potential have to be treated separately. Notice that the Ornstein-Zernike (OZ) equation for the point-like ions can be solved exactly, leading to the Debye-Hückel approximation for bulk electrolytes.

It appeared at that time quite logical to first try to solve the system consisting of two electroneutral subsystems (one quenched and the other annealed) treating ions at the Debye-Hückel level of approximation.[34] Notice that to perform the replica theory calculation, one needs an information about the obstacle (matrix particles) distribution in form of the structure factors (or pair distribution functions) and not the coordinates of the particles. The results, published in ref. 34 were very interesting: it was proved that the interesting effects observed in computer simulations[27] are already present for the point-like ions, that is, at the mean-field level of the approach, leading to the parallel of the Debye-Hückel limiting law for replica systems.

This result paved the road for more sophisticated approaches. In ref. 35–37 the model systems were studied *via* the replica Ornstein-Zernike theory in the hypernetted-chain and the mean-spherical approximations. Both, the matrix and the adsorbed fluid were treated in the primitive model, *i.e.*, the ions were modelled as charged hard spheres embedded in a dielectric continuum. The calculations were later extended to models with uncharged matrix particles and/or highly asymmetrical electrolytes.[36,37] In addition to the structure given by the spatial distribution of particles, some thermodynamical properties were examined. The theory and simulations were recently extended to study the adsorption of ions from electrolyte mixtures.[39]

It was of great interest at that time to establish the validity of the replica Ornstein-Zernike approach for partly-quenched systems with ionic obstacles. Computer simulations for such systems can be time consuming, since the usual canonical averages for the fluid structure must be obtained for a set of realisations of the matrix media.[15,16,27] Further, the computer simulations, in contrast with the theory, require input in terms of the coordinates of the matrix particles. The Monte Carlo simulation results for partly-quenched systems with ionic obstacles were published in ref. 37, 40, 41 and a good agreement was found between the machine calculation and the replica Ornstein-Zernike results.

Thermodynamical properties of electrolytes under confinement caused by the charged or uncharged obstacles are clearly of great interest. The excess internal energy and the compressibility of the adsorbed electrolytes are relatively easy to calculate but these properties are from chemical point of view less interesting than, for example, the excess chemical potential of the invading electrolyte. In the mean-spherical approximation this quantity is relatively easy to calculate.[35] In the hypernetted-chain formalism, the methodology used for bulk fluids[42,43] was successfully extended[37,41] and tested against the Monte Carlo simulation data by some of us. Very interestingly, the hypernetted-chain closure within the replica theory gives (compared to computer simulation results) excellent results, even under conditions[44] where its ''bulk'' version ceases to yield convergent solutions.[38]

Further studies of partly-quenched systems containing charges involve extensions to templated matrices[45] initiated by Zhang and Van Tassel.[46,47] In the same context, an examination of the properties of the water-like fluid in random confinement, published by Urbič and coworkers,[48] should be mentioned. At about the same time Kovalenko and Hirata[49] developed the replica generalisation of the reference interaction site model (replica RISM) integral equation theory to describe the structure and thermodynamics of quenched-annealed systems comprising polar molecular species such as water.

More recently a molecular theory of an electrochemical double layer in a nanoporous carbon supercapacitor was developed by Tanimura, Kovalenko, and Hirata.[50,51] Again, the theory is based on the replica RISM theory of electrolyte solution. The model comprises carbon nanospheres forming a disordered network with the porosity, pore sizes and surface area fitted to carbonised polyvinylidene chloride material and to activated carbon.

Recent developments[52] in both theory and simulation of partly-quenched systems are concerned with the situations where both relevant subsystems (obstacles and annealed electrolyte) are having net charge while, of course, the whole system is electroneutral. Such models mimic, for instance, an adsorption of electrolyte in polyelectrolyte gels and ion-exchangers.

The paper continues with a short section reviewing the systems with directional dependent potentials and partly-quenched systems in external field.

The last sub-chapter of the review is concerned with theoretical description of dynamical properties of electrolyte solutions. Such studies yield an information which is complementary to the thermodynamical data. Here we need to mention the seminal works of Chandler, Chakraborty and others[22,24] who studied the classical diffusion of particles in random media. Monte Carlo simulations of diffusion of ionic particles in charged, disordered media were presented by Mehrabi and Sahimi[53] and commented by Deem.[54] Finally, Dominguez and Rivera[55,56] published a series of molecular dynamics simulation studies of the diffusion of charged fluids in charged porous matrices. The diffusive relaxation of a colloidal fluid adsorbed in a porous medium was studied by Medina–Noyola and coworkers.[57]

The self-diffusion coefficient of ions of the charge- and size-symmetric $+1:-1$ (or $+2:-2$) electrolyte was studied in the presence of ionic obstacles (matrix) representing disordered media by Jardat and coworkers.[58] The study was recently extended to systems mimicking ion-exchangers.[59] The work was stimulated by recent experimental paper of Smith and Zharov[60] who studied the transport of ions through the sulfonated films comprised of silica spheres in water as a function of the ion charge, pH, and solution ionic strength. One of the most recent contribution in this important area of research is due to Rotenberg and coworkers.[61]

At the end, conclusions and perspectives of the rapidly developing field of partly-quenched systems are briefly discussed.

2. Partly-quenched systems

The model used to describe partly-quenched systems consists of two components: one is a quenched fluid, which is called the matrix or adsorbent, and the second is an annealed fluid which thermally equilibrates in the presence of the matrix species. The notation used in this paper is the same as generally used in the literature: the indices 0 and 1 correspond to the matrix and the annealed fluid species, respectively.[7] In the canonical ensemble, the Helmholtz free energy of the partly-quenched system, A, is given by[7,8,27]

$$-\beta A = \ln Z_{\mathrm{TOT}} = \frac{1}{Z'}\int \exp(-\beta_0 \mathscr{H}^{00}) \ln Z_1 \mathrm{d}\mathbf{0} \tag{1}$$

where $\beta = 1/k_\mathrm{B}T$, $\beta_0 = 1/k_\mathrm{B}T_0$ (k_B is the Boltzmann's constant), and Z_{TOT} is the total partition function. Further,

$$Z_1 = \int \exp[-\beta(\mathscr{H}^{01} + \mathscr{H}^{11})]\mathrm{d}\mathbf{1}$$

$$Z' = \int \exp(-\beta_0 \mathscr{H}^{00})\mathrm{d}\mathbf{0}$$

are usual expressions for the partial sums, and $\mathscr{H}^{mn}$ ($m,n = 0,1$) are the Hamiltonians consisting of relevant pairwise interactions. Notation d**0** and d**1** signifies the integration over the coordinates of the quenched and annealed subsystem, respectively. It is important to mention that the temperature of observation of an annealed fluid T does not necessarily coincide with the temperature T_0 at which matrix has been quenched. It is of practical interest to introduce the so-called quenching parameter $Q = \varepsilon_0 T_0/\varepsilon T$, where ε_0 and ε are dielectric constants (relative static permittivities) of the quenched and of the annealed subsystem, respectively.

To solve eqn (1) the replica trick is used.[62,63] The method exploits a mathematical isomorphism between a partly-quenched system and corresponding fully equilibrated system.[8] The properties of the partly-quenched system are obtained by the $s \rightarrow 0$ limit of a replicated system, *i.e.*, a mixture of a one-component fluid (the quenched species) with an s-component fluid, described by s identical copies or replicas of the annealed species

$$\ln Z = \lim_{s\to 0}\frac{1}{s}(Z^s - 1) \tag{2}$$

Substituting eqn (2) into eqn (1) gives for the total partition function

$$\ln Z_{\mathrm{TOT}} = \lim_{s\to 0}\frac{1}{sZ'}\int \left[\exp\left\{-\beta\sum_{i=1}^{s}(\mathscr{H}^{01}_{(i)} + \mathscr{H}^{11}_{(i)})\right\} - 1\right]\exp(-\beta_0\mathscr{H}^{00})\mathrm{d}\mathbf{1}\mathrm{d}\mathbf{0} \tag{3}$$

The total partition function given by eqn (3) belongs to a system described by the following Hamiltonian

$$\mathscr{H} = \sum_{i<j} U^{00}(r) + \sum_{i,j} U^{01}(r) + \sum_{i<j} U^{11}(r)\delta_{\sigma_i\sigma_j} \tag{4}$$

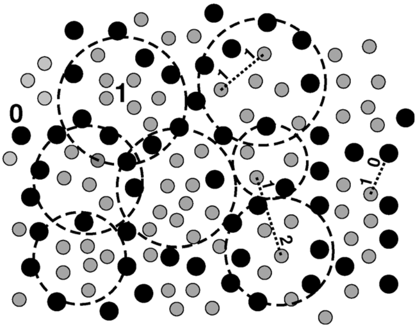

Fig. 1 To give a pictorial explanation of the correlations included in the connecting and blocking parts of the correlation functions, we imagine the partly-quenched system as a fluid adsorbed in a porous material with the porous material being constituted by the quenched particles (black circles–"0") and the fluid being constituted by the annealed particles (grey circles–"1"). The connected functions (denoted "11" in the figure) account for correlations between a pair of fluid particles that are transmitted through successive layers of fluid particles within the same "replica", and the blocking functions (denoted "12") account for the correlations between fluid particles "blocked" or separated from each other by matrix particles, *e.g.*, fluid particles from different "replicas" (dashed circles).

where $\delta_{\sigma_i \sigma_j}$ is the Kronecker delta function, σ_i denotes the replicated component to which particle i belongs, and $U^{mn}(r)$ $(m,n = 0,1)$ denotes the interaction potential between particles i and j separated by a distance r. The Hamiltonian belongs to a mixture of a one component fluid (0) with the s-component fluid in which particles interact with each other only if they belong to the same replicated component. Particles belonging to different replicas only correlate through particles 0 (see Fig. 1).

Note that this so-called "replica" method was originally developed to treat model systems on a lattice in which the exchange interaction strength between lattice sites was chosen from a fixed random distribution.[63,64] The liquid-state replica method, or "continuous replica", that is being reviewed in this paper, on the other hand, is applied to systems in which some of the particles have been quenched or "frozen" in an equilibrium distribution corresponding to a temperature of a quench.[7,8,65]

(a) Computer simulation approach

The simulation procedures developed to study the partly-quenched systems in general combine two processes. First, the matrix is prepared in advance in a separate simulation by equilibrating the subsystem at temperature T_0. The Monte Carlo simulation method or molecular dynamics simulation can be used for this purpose. After the equilibration procedure the particles are frozen in their positions; the particle distribution represents one of the possible equilibrium configurations. The annealed fluid is then distributed within the (matrix) system at temperature T, without imposing any effect on the matrix structure, *i.e.*, the distribution of obstacles remains unaffected. During the simulation, the thermodynamical properties of the annealed fluid are calculated as ensemble averages over different fluid configurations. Since the properties of the partly-quenched systems are actually given as double averages, *e.g.*, over the annealed fluid and over possible matrix configurations, the procedure is repeated for other matrix realisations in order to obtain the matrix average. In practise, usually only few matrix configurations are sufficient[17,22,37,66] to obtain the convergent result.

An exception to this simulation scheme is the work of Bratko and Chakraborty.[27] In the latter simulation, the properties of dilute annealed electrolyte at the finite matrix concentration were studied using the Widom's insertion technique, performing the two processes (averaging over the fluid and the matrix configurations) simultaneously. The matrix was equilibrated at temperature T_0 using the canonical Monte Carlo simulation. For each matrix configuration, several insertions of a neutral combination of the annealed fluid ions were attempted at temperature T.

(b) Integral equation theory

The first attempt to develop an integral equation theory for partly-quenched systems was, to best of our knowledge, the work of Madden and Glandt.[4,5] They used the graph theory to develop and analyse the cluster expansion of the total, $h^{11}(r)$, and the direct correlation functions, $c^{11}(r)$. In the process, both functions were divided into the "connected" part ("c"), representing the interaction within the same replica, and "blocking" part ("b"), describing interactions mediated by the matrix particles. In the graph theory, this is a subset of graphs in which all paths between the annealed fluid root points pass through at least one matrix point.[4,5] In their seminal work, Madden and Glandt proposed the approximation: $c^{11,\mathrm{b}}(r) = 0$, and obtained an Ornstein-Zernike-like set of equations describing the partly-quenched systems.

The exact equations for such systems, relaxing the approximation above, were later proposed by Given and Stell.[7,8] Using the notation common in the literature, and introducing $c^{11,\mathrm{b}}(r) = c^{12}(r)$, and $h^{11,\mathrm{b}}(r) = h^{12}(r)$, the equations read[8]

$$\begin{aligned}
\mathbf{H}^{00} - \mathbf{C}^{00} &= \mathbf{C}^{00} \otimes \boldsymbol{\rho}^0\mathbf{H}^{00} + s\mathbf{C}^{01} \otimes \boldsymbol{\rho}^1\mathbf{H}^{10}\\
\mathbf{H}^{10} - \mathbf{C}^{10} &= \mathbf{C}^{10} \otimes \boldsymbol{\rho}^0\mathbf{H}^{00} + \mathbf{C}^{11} \otimes \boldsymbol{\rho}^1\mathbf{H}^{10} + (s-1)\mathbf{C}^{12} \otimes \boldsymbol{\rho}^1\mathbf{H}^{10}\\
\mathbf{H}^{11} - \mathbf{C}^{11} &= \mathbf{C}^{10} \otimes \boldsymbol{\rho}^0\mathbf{H}^{01} + \mathbf{C}^{11} \otimes \boldsymbol{\rho}^1\mathbf{H}^{11} + (s-1)\mathbf{C}^{12} \otimes \boldsymbol{\rho}^1\mathbf{H}^{21}\\
\mathbf{H}^{12} - \mathbf{C}^{12} &= \mathbf{C}^{10} \otimes \boldsymbol{\rho}^0\mathbf{H}^{01} + \mathbf{C}^{11} \otimes \boldsymbol{\rho}^1\mathbf{H}^{12} + \mathbf{C}^{12} \otimes \boldsymbol{\rho}^1\mathbf{H}^{11} + (s-2)\mathbf{C}^{12} \otimes \boldsymbol{\rho}^1\mathbf{H}^{21}
\end{aligned} \tag{5}$$

The capital letters $\mathbf{H}^{mn}$ and $\mathbf{C}^{mn}$ ($m,n = 0,1,2$) denote the matrix forms of the correlation functions, $h^{mn}(r)$ and $c^{mn}(r)$, respectively, and the symbol $\otimes$ denotes convolution in r-space. In the limit $s \to 0$, one obtains the so-called replica Ornstein-Zernike equations (ROZ)[8]

$$\begin{aligned}
\mathbf{H}^{00} - \mathbf{C}^{00} &= \mathbf{C}^{00} \otimes \boldsymbol{\rho}^0\mathbf{H}^{00}\\
\mathbf{H}^{10} - \mathbf{C}^{10} &= \mathbf{C}^{10} \otimes \boldsymbol{\rho}^0\mathbf{H}^{00} + \mathbf{C}^{11} \otimes \boldsymbol{\rho}^1\mathbf{H}^{10} - \mathbf{C}^{12} \otimes \boldsymbol{\rho}^1\mathbf{H}^{10}\\
\mathbf{H}^{11} - \mathbf{C}^{11} &= \mathbf{C}^{10} \otimes \boldsymbol{\rho}^0\mathbf{H}^{01} + \mathbf{C}^{11} \otimes \boldsymbol{\rho}^1\mathbf{H}^{11} - \mathbf{C}^{12} \otimes \boldsymbol{\rho}^1\mathbf{H}^{21}\\
\mathbf{H}^{12} - \mathbf{C}^{12} &= \mathbf{C}^{10} \otimes \boldsymbol{\rho}^0\mathbf{H}^{01} + \mathbf{C}^{11} \otimes \boldsymbol{\rho}^1\mathbf{H}^{12} + \mathbf{C}^{12} \otimes \boldsymbol{\rho}^1\mathbf{H}^{11} - 2\mathbf{C}^{12} \otimes \boldsymbol{\rho}^1\mathbf{H}^{21}
\end{aligned} \tag{6}$$

For electrolyte solutions, $\mathbf{H}^{mn}$ and $\mathbf{C}^{mn}$ are matrices of dimension at least 2×2. Note that in eqn (7) and (18) the matrices are explicitly written for the case of a single electrolyte in an electroneutral electrolyte matrix. In this case, the matrices contain $++$, $+-$, $-+$, and $--$ functions, and $\boldsymbol{\rho}^i$ has the form[67]

$$\begin{pmatrix} \rho^i_+ & 0 \\ 0 & \rho^i_- \end{pmatrix} \tag{7}$$

The total correlation functions, $h^{11}(r)$, and the direct correlation functions, $c^{11}(r)$, contained in the matrices are divided into the connecting (“c”) and blocking (“b”) parts, respectively[8]

$$
\begin{aligned}
c^{11}(r) &= c^{11,\mathrm{c}}(r) + c^{11,\mathrm{b}}(r) = c^{11,\mathrm{c}}(r) + c^{12}(r)\\
h^{11}(r) &= h^{11,\mathrm{c}}(r) + h^{11,\mathrm{b}}(r) = h^{11,\mathrm{c}}(r) + h^{12}(r)
\end{aligned}
\tag{8}
$$

The set of integral equations presented above, eqn (6), can only be solved with additional approximations: the so-called closure conditions. In contrast to a bulk electrolyte, where only approximations for $c^{00}(r)$, $c^{10}(r)$ and $c^{11}(r)$ are required, we need here additional equations to approximate the blocking part $c^{12}(r)$ of the direct correlation functions. For bulk ionic systems, two closure relations–the so-called mean spherical approximation (MSA) and the hypernetted-chain (HNC) approximation–are widely used and represent a natural choice also in our example. Each of these two closures has its advantages and disadvantages. The HNC approximation has proved to be very successful for ionic fluids, and can even be improved by including the so-called bridge functions.[14,68] In addition, the HNC approximation is consistent with the ROZ methodology while, in contrast, in the MSA the blocking term of the direct correlation function, $c^{12}(r)$, is neglected.[35] There is one advantage of the latter closure: it appears to be easier to evaluate the thermodynamical properties of quenched-annealed systems within the MSA formalism.[19]

The HNC closure relations are given by[35]

$$
\begin{aligned}
c^{mn}(r) &= \exp[-\beta U^{mn}(r)] + \gamma^{mn}(r)] - 1 - \gamma^{mn}(r)\\
c^{12}(r) &= \exp[\gamma^{12}(r)] - 1 - \gamma^{12}(r)
\end{aligned}
\tag{9}
$$

where $\gamma^{mn}(r) = h^{mn}(r) - c^{mn}(r)$ and the superscripts m,n assuming values 0 and 1. $U^{mn}(r)$ are the inter-particle potentials for different components.

The MSA closure sets $c^{12}(r)$ to zero and consequently we have[69]

$$
\begin{aligned}
h^{mn}(r) &= -1, \quad r < (\sigma_m + \sigma_n)/2\\
c^{mn}(r) &= -\beta U^{mn}(r), \quad r \geq (\sigma_m + \sigma_n)/2
\end{aligned}
\tag{10}
$$

where again the superscripts m,n assume values of 0 and 1, and σ_m, σ_n are the diameters of the species m and n, respectively. Note that setting the blocking part of the direct correlation function to zero does not imply that there is no correlation between the particles belonging to different replicas. As shown in ref. 34, the blocking part of the total correlation function, $h^{12}(r)$, remains to be nonzero in such a case.

Dilute electrolyte solutions are most often described by the primitive model, where the particle-particle interaction is

$$
U_{ij}^{00}(r) = \begin{cases} \infty, & r < (\sigma_i^0 + \sigma_j^0)/2\\ \frac{e^2 z_i^0 z_j^0}{4\pi\varepsilon'\varepsilon_0 r}, & r \geq (\sigma_i^0 + \sigma_j^0)/2 \end{cases}
\tag{11}
$$

and

$$U_{ij}^{10}(r) = \begin{cases} \infty, & r < (\sigma_i^1 + \sigma_j^0)/2 \\ \frac{e^2 z_i^1 z_j^0}{4\pi\varepsilon'\varepsilon r}, & r \geq (\sigma_i^1 + \sigma_j^0)/2 \end{cases} \tag{12}$$

$$U_{ij}^{11}(r) = \begin{cases} \infty, & r < (\sigma_i^1 + \sigma_j^1)/2 \\ \frac{e^2 z_i^1 z_j^1}{4\pi\varepsilon'\varepsilon r}, & r \geq (\sigma_i^1 + \sigma_j^1)/2 \end{cases} \tag{13}$$

In eqn (11)–(13) e denotes the elementary charge, z_i^m (z_j^m) the charge numbers (valencies) of ions (m = 0,1), ε' the permittivity of vacuum, ε_0 and ε the dielectric constants of the pre-quenching conditions and of the studied partly-quenched system, respectively, σ_i^0 and σ_i^1 the diameters of the matrix and of the fluid particles, respectively, and as usual r denotes the distance between particles i and j. Note that setting the charge numbers z_i^0 and z_j^0 in eqn (11) and (12) to zero, we obtain the expression valid for matrix composed of uncharged hard spheres.[37]

To continue, we need to develop a re-normalisation scheme for the long-range terms of ion–ion correlations. The procedure was for the bulk electrolytes described in details elsewhere (see, for example ref. 38, 67, 68, 70). However, to solve the ROZ/HNC or the ROZ/MSA equations, some modifications are needed.

Similarly to previous such studies, we denote the long-range terms of the total pair correlation functions in eqn (6) by $q_{ij}^{mn}(r)$. Moreover, we apply the linearised theory and assume that the long-range terms of the direct correlation functions contained in the matrices $\mathbf{\Phi}^{mn}$ are equal to $\varphi_{ij}^{mn}(r)$[35]

$$\begin{aligned} \mathbf{C}^{mm} &= \mathbf{C}_{(s)}^{mm} + \mathbf{\Phi}^{mm} \\ \mathbf{C}^{0m} &= \mathbf{C}_{(s)}^{0m} + \mathbf{\Phi}^{0m} \\ \mathbf{C}^{12} &= \mathbf{C}_{(s)}^{12} \end{aligned} \tag{14}$$

and

$$\mathbf{H}^{mn} = \mathbf{H}_{(s)}^{mn} + \mathbf{q}^{mn} \tag{15}$$

where the superscripts m,n assume the values 0,1,2 and subscript (s) denotes the short-range part of the correlation functions. $\mathbf{q}^{mn}$ is the matrix containing the long-range parts of the total correlation functions $\mathbf{q}_{ij}^{mn}(r)$. Further, $\mathbf{C}^{22} = \mathbf{C}^{11}$, $\mathbf{C}^{01} = \mathbf{C}^{02}$, $\mathbf{H}^{22} = \mathbf{H}^{11}$, $\mathbf{\Phi}^{22} = \mathbf{\Phi}^{11}$. Most importantly, since the particles belonging to different replicas do not interact, $\mathbf{\Phi}^{12} = \mathbf{0}$.We now choose the elements $\varphi_{ij}^{mn}(r)$ of the matrix $\mathbf{\Phi}^{mn}$ in the form of the Coulomb interaction[35]

$$\begin{aligned} \varphi_{ij}^{mn}(r) &= -\frac{e^2 z_i^m z_j^n}{4\pi\varepsilon'\varepsilon r k_B T} \\ \varphi_{ij}^{00}(r) &= -\frac{e^2 z_i^0 z_j^0}{4\pi\varepsilon'\varepsilon_0 r k_B T_0} \end{aligned} \tag{16}$$

Functions $\mathbf{q}^{mn}$ are further chosen to satisfy the following equations[34]

$$\mathbf{q}^{00} - \mathbf{\Phi}^{00} = \mathbf{\Phi}^{00} \otimes \boldsymbol{\rho}^0 \mathbf{q}^{00}$$

$$\mathbf{q}^{10} - \mathbf{\Phi}^{10} = \mathbf{\Phi}^{10} \otimes \boldsymbol{\rho}^0 \mathbf{q}^{00} + \mathbf{\Phi}^{11} \otimes \boldsymbol{\rho}^1 \mathbf{q}^{10}$$

$$\begin{aligned}\mathbf{q}^{11} - \boldsymbol{\Phi}^{11} &= \boldsymbol{\Phi}^{10} \otimes \boldsymbol{\rho}^{0}\mathbf{q}^{01} + \boldsymbol{\Phi}^{11} \otimes \boldsymbol{\rho}^{1}\mathbf{q}^{11} \\ \mathbf{q}^{12} - \boldsymbol{\Phi}^{12} &= \boldsymbol{\Phi}^{10} \otimes \boldsymbol{\rho}^{0}\mathbf{q}^{01} + \boldsymbol{\Phi}^{11} \otimes \boldsymbol{\rho}^{1}\mathbf{q}^{12}\end{aligned} \tag{17}$$

The set of eqn (17) can be readily solved to obtain the Fourier transforms of the screened potentials.[34] The expressions in Cartesian space follow then straightforwardly[36]

$$\begin{aligned}\begin{pmatrix} q^{00}_{++}(r) & q^{00}_{+-}(r) \\ q^{00}_{-+}(r) & q^{00}_{--}(r)\end{pmatrix} &= -\frac{L_B}{Q}\begin{pmatrix} z^0_+z^0_+ & z^0_+z^0_- \\ z^0_-z^0_+ & z^0_-z^0_-\end{pmatrix}\frac{\exp(-\kappa_0 r)}{r} \\ \begin{pmatrix} q^{10}_{++}(r) & q^{10}_{+-}(r) \\ q^{10}_{-+}(r) & q^{10}_{--}(r)\end{pmatrix} &= -L_B\frac{\kappa_0^2}{\kappa_0^2-\kappa_1^2}\begin{pmatrix} z^1_+z^0_+ & z^1_+z^0_- \\ z^1_-z^0_+ & z^1_-z^0_-\end{pmatrix} \\ &\times\left[\frac{\exp(-\kappa_0 r)}{r} - \frac{\kappa_1^2}{\kappa_0^2}\frac{\exp(-\kappa_1 r)}{r}\right]\end{aligned}$$

$$\begin{aligned}\begin{pmatrix} q^{12}_{++}(r) & q^{12}_{+-}(r) \\ q^{12}_{-+}(r) & q^{12}_{--}(r)\end{pmatrix} &= 2\pi L_B^2\frac{\rho^0_+(z^0_+)^2+\rho^0_-(z^0_-)^2}{\kappa_0^2-\kappa_1^2} \\ &\times\left\{-\frac{2\kappa_0^2\exp(-\kappa_0 r)}{r(\kappa_0^2-\kappa_1^2)} + \frac{2\kappa_0^2\exp(-\kappa_1 r)}{r(\kappa_0^2-\kappa_1^2)} - \kappa_1\exp(-\kappa_1 r)\right\} \\ &\times\begin{pmatrix} z^1_+z^1_+ & z^1_+z^1_- \\ z^1_-z^1_+ & z^1_-z^1_-\end{pmatrix} \\ \begin{pmatrix} q^{11}_{++}(r) & q^{11}_{+-}(r) \\ q^{11}_{-+}(r) & q^{11}_{--}(r)\end{pmatrix} &= -L_B\begin{pmatrix} z^1_+z^1_+ & z^1_+z^1_- \\ z^1_-z^1_+ & z^1_-z^1_-\end{pmatrix}\frac{\exp(-\kappa_1 r)}{r} + \begin{pmatrix} q^{12}_{++}(r) & q^{12}_{+-}(r) \\ q^{12}_{-+}(r) & q^{12}_{--}(r)\end{pmatrix}\end{aligned} \tag{18}$$

where $\kappa_0 = (\Sigma_i\rho^0_i(z^0_i)^2L_B/Q)^{1/2}$, $\kappa_1 = (\Sigma_i\rho^1_i(z^1_i)^2L_B/Q)^{1/2}$ and $L_B = e^2/(4\pi\varepsilon'\varepsilon k_BT)$.

Finally, the ROZ equations can be rewritten in the re-normalised form.[36] As a first expression, we present the equation for the matrix subsystem

$$\mathbf{H}^{00}_{(s)} - \mathbf{C}^{00}_{(s)} = \mathbf{C}^{00}_{(s)} \otimes \boldsymbol{\rho}^{0}(\mathbf{H}^{00}_{(s)} + \mathbf{q}^{00}) + \boldsymbol{\Phi}^{00} \otimes \boldsymbol{\rho}^{0}\mathbf{H}^{00}_{(s)} \tag{19}$$

and continue with the others

$$\begin{aligned}\mathbf{H}^{10}_{(s)} - \mathbf{C}^{10}_{(s)} &= \mathbf{C}^{10}_{(s)} \otimes \boldsymbol{\rho}^{0}(\mathbf{H}^{00}_{(s)} + \mathbf{q}^{00}) + \boldsymbol{\Phi}^{10} \otimes \boldsymbol{\rho}^{0}\mathbf{H}^{00}_{(s)} + \mathbf{C}^{11}_{(s)}\otimes \boldsymbol{\rho}^{1}(\mathbf{H}^{10}_{(s)} + \mathbf{q}^{10}) \\ &+ \boldsymbol{\Phi}^{11} \otimes \boldsymbol{\rho}^{1}\mathbf{H}^{10}_{(s)} - \mathbf{C}^{12}_{(s)}\otimes \boldsymbol{\rho}^{1}(\mathbf{H}^{10}_{(s)} + \mathbf{q}^{10}) \\ \mathbf{H}^{11}_{(s)} - \mathbf{C}^{11}_{(s)} &= \mathbf{C}^{10}_{(s)} \otimes \boldsymbol{\rho}^{0}(\mathbf{H}^{01}_{(s)} + \mathbf{q}^{01}) + \boldsymbol{\Phi}^{10} \otimes \boldsymbol{\rho}^{0}\mathbf{H}^{01}_{(s)} + \mathbf{C}^{11}_{(s)}\otimes \boldsymbol{\rho}^{1}(\mathbf{H}^{11}_{(s)} + \mathbf{q}^{11}) \\ &+ \boldsymbol{\Phi}^{11} \otimes \boldsymbol{\rho}^{1}\mathbf{H}^{11}_{(s)} - \mathbf{C}^{12}_{(s)}\otimes \boldsymbol{\rho}^{1}(\mathbf{H}^{21}_{(s)} + \mathbf{q}^{21}) \\ \mathbf{H}^{12}_{(s)} - \mathbf{C}^{12}_{(s)} &= \mathbf{C}^{10}_{(s)} \otimes \boldsymbol{\rho}^{0}(\mathbf{H}^{01}_{(s)} + \mathbf{q}^{01}) + \boldsymbol{\Phi}^{10} \otimes \boldsymbol{\rho}^{0}\mathbf{H}^{01}_{(s)} + \mathbf{C}^{11}_{(s)}\otimes \boldsymbol{\rho}^{1}(\mathbf{H}^{12}_{(s)} + \mathbf{q}^{12}) \\ &+ \boldsymbol{\Phi}^{11} \otimes \boldsymbol{\rho}^{1}\mathbf{H}^{12}_{(s)} - \mathbf{C}^{12}_{(s)}\otimes \boldsymbol{\rho}^{1}\mathbf{H}^{11}_{(s)} - 2\mathbf{C}^{12}_{(s)}\otimes \boldsymbol{\rho}^{1}\mathbf{H}^{21}\end{aligned} \tag{20}$$

(c) Thermodynamical properties

Calculating thermodynamical properties of the partly-quenched system we have to be aware that the standard statistical-mechanical expressions used for bulk solutions, such as virial equation of state, may not be valid any more. In principle, all the thermodynamical parameters have to be re-derived within the replica formalism in a similar way as, for example, the replica Ornstein-Zernike equations given in section 2b. The thermodynamical equations for the partly-quenched systems were formally introduced by Ford and Glandt,[17] and Rosinberg *et al.*[13] A thorough analysis of thermodynamical properties of partly-quenched systems was performed by Given.[6] He developed the Mayer expansion for the thermodynamical quantities of an adsorbed fluid, as well as discussed the relationships between correlation functions and thermodynamical quantities that hold for such systems. Although the calculation of some thermodynamical properties, such as the excess internal energy and the isothermal compressibility, are quite straightforward, other equations presented, such as the Gibbs-Duhem-like equation, are of little practical application.

The excess internal energy, E^{ex}, of a charged fluid per annealed particle (N_1) inside a charged matrix ($\beta = 1/k_{\mathrm{B}}T$) can be calculated as[19]

$$\begin{aligned}\frac{\beta E^{\mathrm{ex}}}{N_1} &= \frac{1}{2}\sum_{i=+,-}\sum_{j=+,-} x_i^1\rho_j^1 \int g_{ij}^{11}(r)U_{ij}^{11}(r)\mathrm{d}\mathbf{r}\\ &\quad+\sum_{i=+,-}\sum_{j=+,-} x_i^1\rho_j^0 \int g_{ij}^{10}(r)U_{ij}^{10}(r)\mathrm{d}\mathbf{r}\end{aligned} \tag{21}$$

where $x_i^1 = \rho_i^1/\Sigma_i\rho_i^1$ denotes the mole fraction of the annealed species, $g_{ij}^{mn}(r) = h_{ij}^{mn}(r) + 1$ is the radial distribution function, U_{ij}^{mn} the pair potential ($m,n = 0,1$), and $\mathrm{d}\mathbf{r} = 4\pi r^2\mathrm{d}\mathbf{r}$.

Another well established relation is the equation for the inverse value of the reduced isothermal compressibility, which reads[13]

$$\left(\frac{\partial\beta P}{\partial\rho_1}\right)_T = 1-\rho_1\sum_{i=+,-}\sum_{j=+,-} x_i^1 x_j^1\int[c_{(\mathrm{s})ij}^{11}(r)-c_{(\mathrm{s})ij}^{12}(r)]\mathrm{d}\mathbf{r} \tag{22}$$

P denotes the pressure of the system, $c_{(\mathrm{s})ij}^{mn}(r)$ is the short-range part of the direct correlation function and $\rho_1 = \Sigma_i\rho_i^1$.

The excess chemical potential is of primary importance for the description of the adsorption isotherms. Within the MSA this quantity can be approximated by[19]

$$\begin{aligned}\beta\mu_i^{\mathrm{ex}} &= \beta\mu_i^{\mathrm{ex,r}}+\frac{1}{2}\beta\sum_{j=+,-}\rho_j^1\int g_{ij}^{11}(r)U_{ij}^{11}(r)\mathrm{d}\mathbf{r}\\ &\quad+\frac{1}{2}\beta\sum_{j=+,-}\rho_j^0\int g_{ij}^{10}(r)U_{ij}^{10}(r)\mathrm{d}\mathbf{r}\\ &\quad-\sum_{j=+,-}\rho_j^1\int[c_{(\mathrm{s})ij}^{11}(r)-c_{(\mathrm{r})ij}^{11}(r)]\mathrm{d}\mathbf{r}\\ &\quad-\sum_{j=+,-}\rho_j^0\int[c_{(\mathrm{s})ij}^{10}(r)-c_{(\mathrm{r})ij}^{10}(r)]\mathrm{d}\mathbf{r}\end{aligned} \tag{23}$$

$c_{(\mathrm{r})ij}^{mn}(r)$ stands for the direct correlation functions for the reference system. Very often a hard sphere fluid in a hard sphere matrix is chosen as the reference system. The reduced chemical potential of the reference system, $\beta\mu_i^{\mathrm{ex,r}}$, was obtained by integration of the compressibility equation[13,17]

$$\begin{aligned}\beta\mu_i^{\mathrm{ex,r}}(\rho_0,\rho_1) &= \beta\mu_i^{\mathrm{ex,r}}(\rho_0,\rho_+^1=0,\rho_-^1=0)\\ &\quad-\sum_{j=+,-}\int_0^{\rho_1/2}\mathrm{d}(\rho_j^1)'\int c_{(\mathrm{r})ij}^{11}(r,(\rho_+^1)',(\rho_-^1)')\mathrm{d}\mathbf{r}\end{aligned} \tag{24}$$

Note that eqn (24) is written for a symmetric electrolyte where $\rho^1_+ = \rho^1_- = \rho_1/2$. In the case where $\sigma^0_+ = \sigma^0_+ = \sigma_0$, the expression for $\beta\mu^{\mathrm{ex,r}}_+(\rho_0,\rho^1_+ = 0,\rho^1_- = 0)$ follows from the Mansoori-Carnahan-Starling-Leland equation of state[71,72]

$$\beta\mu^{\mathrm{ex,r}}_+(\rho_0,\rho^1_+ = 0,\rho^1_- = 0) = \frac{3\eta_0^3 - 9\eta_0^2 + 8\eta_0}{(1-\eta_0)^3} \tag{25}$$

where η_0 denotes the packing fraction, defined as $\eta_0 = \pi\rho_0\sigma_0^3/6$.

Another route to calculate the excess chemical potential of electrolytes, valid for bulk electrolytes within the HNC approximation, was proposed by Belloni.[42,43] The expression was re-derived by us within the replica formalism and reads[37]

$$\begin{aligned}\beta\mu^{\mathrm{ex}}_{i,1} = & -\sum_{j=+,-}\rho_j^0\mathbf{c}^{\mathbf{10}}_{\mathbf{(s)ij}}(0) - \sum_{j=+,-}\rho_j^1[\mathbf{c}^{\mathbf{11}}_{\mathbf{(s)ij}}(0) - \mathbf{c}^{\mathbf{12}}_{\mathbf{(s)ij}}(0)] \\ & + \frac{1}{2}\sum_{j=+,-}\rho_j^0\int h_{ij}^{10}(r)[h_{ij}^{10}(r) - c_{ij}^{10}(r)]\mathrm{d}\mathbf{r} \\ & + \frac{1}{2}\sum_{j=+,-}\rho_j^1\int \{h_{ij}^{11}(r)[h_{ij}^{11}(r) - c_{ij}^{11}(r)] - h_{ij}^{12}(r)[h_{ij}^{12}(r) - c_{ij}^{12}(r)]\}\mathrm{d}\mathbf{r}\end{aligned} \tag{26}$$

where $\mathbf{c}^{\mathbf{mn}}_{\mathbf{(s)ij}}(0)$ denotes the Fourier transform of the short-range part of the direct correlation function at $k = 0$. As we will show later, this extension of the equation for the excess chemical potential proved to be extremely valuable; the expression for $\mu^{\mathrm{ex}}_{i,1}$ proposed (eqn (26)) is accurate and simple to use.

3. Case studies

Bratko and Chakraborty[27] used the Monte Carlo simulation method to study the influence of the matrix consisting of a quenched electrolyte on the properties of the dilute ionic fluid at temperatures different from the temperature of the quench. The characteristic quantity of the ionic disordered material, the quenching parameter $Q = \varepsilon_0 T_0/\varepsilon T$, was introduced. Focusing on the characteristic properties, such as the distribution functions and the chemical potential of the solute they noticed qualitative differences between the partly-quenched and fully annealed fluids under similar conditions of observation. They ascribed these differences to the influence of the presence of fixed obstacles being prepared under different conditions (T_0, ε_0) from the conditions of observation. If the product $\varepsilon_0 T_0$ exceeds the corresponding value at the conditions of observation, εT, ($Q > 1$) the electrostatic potential fluctuations will be stronger than expected in an equilibrated ionic mixture at εT, and the solute ions will typically find themselves in oppositely charged domains with the net charge exceeding their own charge. The resulting over-screening of the solute charge leads to a long-ranged disorder-induced attraction between equally charged ions and a similar mechanism induces a long-ranged repulsive interaction between ionic solutes of opposite sign (Fig. 2c). A similar effect was noticed in solutions of highly asymmetric electrolytes in the presence of divalent counterions.[73] If, on the other hand, $\varepsilon_0 T_0 < \varepsilon T$, ($Q < 1$) the solute ions remain under-screened (Fig. 2a). In the latter case, a long-ranged interaction representing a fraction of the direct Coulomb potential between the solute ions remains unscreened. The

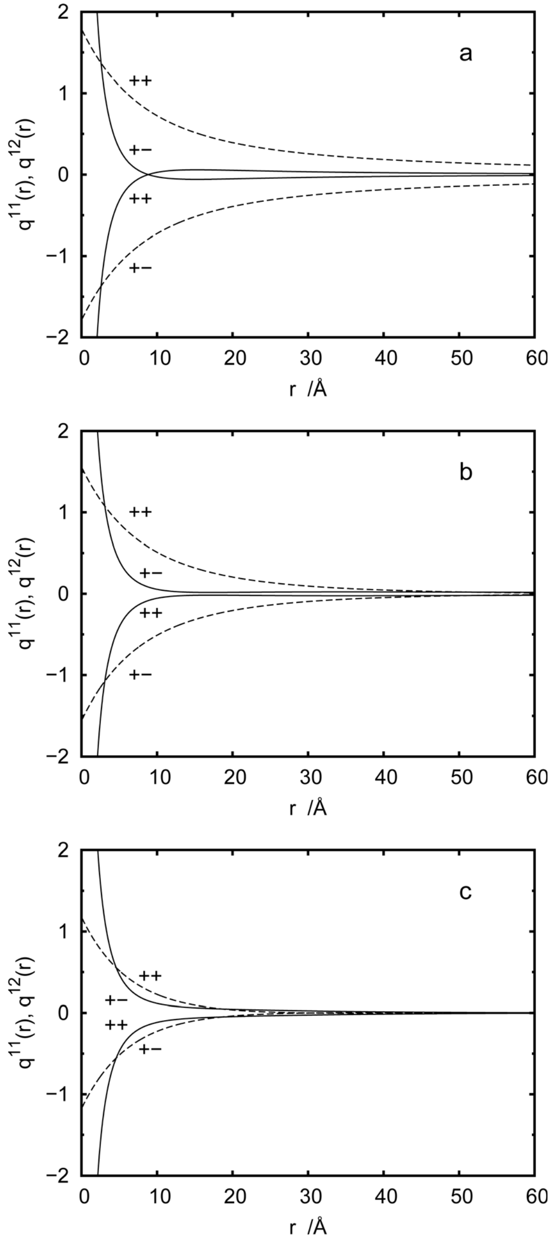

Fig. 2 The Debye-Hückel-like level of the ROZ theory. The screened potentials of the fluid ion–ion interaction, $q^{11}(r)$ (continuous lines), and their blocking parts, $q^{12}(r)$ (dashed lines), all calculated using the eqn (18), at different values of the quenching parameter: $Q = 0.7$ (panel a), $Q = 1.0$ (panel b), and $Q = 1.7$ (panel c). The matrix and the fluid are $+1 : -1$ electrolytes with concentrations $c_0 = 0.01$ mol dm^{-3}, and $c_1 = 0.1$ mol dm^{-3}, respectively. $L_B = 7.14$ Å. A similar figure but for a different set of parameters was previously presented in ref. 34.

simulation results therefore reveal a crucial effect of Q not just on the annealed fluid structure but also on solution energies and on the activity coefficients of the solute particles.[27]

(a) The Debye-Hückel-like level of the ROZ theory

Before we start this and other sections, we have to stress that the numerical results presented in this article, obtained *via* the integral equation theory, were not taken from previous papers but were rather calculated from scratch. The speed of nowadays computers allowed us better numerical accuracy in solving the ROZ equations than it could be obtained a decade ago. Yet, we did not notice any disagreements between the old and new results, wherever exactly the same input parameters were used. This made it possible to re-plot all the figures published before, using the new data. In few cases, also the computer simulations were repeated; wherever we used the old simulation results this is clearly mentioned in the caption to the figure (*i.e.*, Fig. 7, 9–11).

Although there were previous attempts to apply the ROZ equations to study the partly-quenched ionic fluids by Pastore *et al.*,[74] and Cardenas and Tosi,[75] the first systematic integral equation study of liquids, described by the Coulomb potential in charged matrices, based on the correct closure, was initiated by Pizio and coworkers.[34,35] In their first paper,[34] the ROZ equations were utilised to study the ionic fluid adsorbed in an electroneutral disordered matrix, where both ionic subsystems were presented as point charges interacting *via* classical Coulomb potential. We shall denote this approach as the Debye-Hückel-like level of approximation.

It was shown[34] that the peculiar behaviour, described with the terms "over-" and "under-screening", observed in computer simulations,[27] follows straightforwardly from the ROZ equations already on the simplest mean-field level of approach. One example of such behaviour is shown in Fig. 2, where the screened potentials of the fluid ion–ion interaction, $q^{11}(r)$ (continuous lines), and their blocking parts, $q^{12}(r)$ (dashed lines), are presented for different values of the quenching parameter: $Q = 0.7$ (panel a), $Q = 1.0$ (panel b), and $Q = 1.7$ (panel c). The matrix and the fluid are both pictured as $+1:-1$ electrolytes with concentrations $c_0 = 0.01$ mol dm^{-3}, and $c_1 = 0.1$ mol dm^{-3}, respectively. Note that a similar figure, but for different set of parameters was previously presented in ref. 34. The results presented here are showing same qualitative behaviours as in the original paper.[34] In all cases, the annealed electrolyte was considered to be an aqueous solution at $T = 298.15$ K (corresponding Bjerrum length equals $L_B = 7.14$ Å), and the temperature of the quench, T_0, was determined by the quenching parameter Q. The results are consistent with those obtained by computer simulations.[27] An interesting observation, which was not shown by computer simulations, is the fact that the blocking functions, $q^{12}(r)$, have an opposite sign to their 11 counterparts, leading to faster decay of $q^{11}_{+-}(r)$, and faster augmenting of $q^{11}_{++}(r)$.[34]

Hribar *et al.*[34] systematically investigated the influence of the fluid and the matrix concentrations to the structure of the annealed fluid. Fig. 3 is showing the screened potentials of the fluid ion–ion interaction, $q^{11}(r)$ (continuous lines), and their blocking parts, $q^{12}(r)$ (dashed lines), at a single quenching parameter, $Q = 1.2$, and different values of the annealed fluid concentration: $c_1 = 5 \times 10^{-5}$ mol dm^{-3} (panel a), 5×10^{-3} mol dm^{-3} (panel b), and 5×10^{-2} mol dm^{-3} (panel c). Again, the matrix and the fluid are $+1:-1$ electrolytes and the matrix concentration is $c_0 = 0.5$ mol dm^{-3}. The functions shown in Fig. 3 were for different set of parameters presented first in ref. 34. However, the same qualitative trends were observed. Similar type of behaviour as triggered by different pre-quenching conditions is here observed as a consequence of different fluid concentration. While at low annealed fluid concentration (Fig. 3a) strong effect of the blocking term on the behaviour of

$q^{11}(r)$ is observed, the influence of the matrix ions diminishes with the increasing fluid concentration. At high concentrations, the fluid behaves similar as a matrix-free (bulk) electrolyte solution (Fig. 3c).[34]

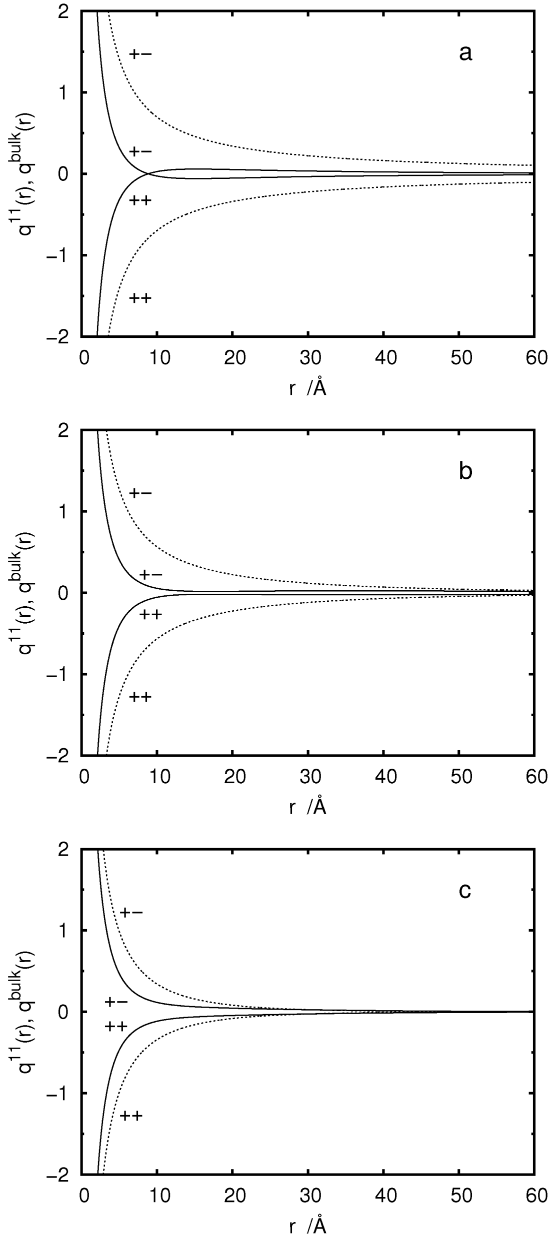

Fig. 3 The Debye-Hückel-like level of the ROZ theory. The screened potentials of the fluid ion–ion interaction, $q^{11}(r)$ (continuous lines), and their blocking parts, $q^{12}(r)$ (dashed lines), calculated using eqn (18), at different values of the annealed fluid concentration: $c_1 = 5 \times 10^{-5}$ mol dm^{-3} (panel a), 5×10^{-3} mol dm^{-3} (panel b), and 5×10^{-2} mol dm^{-3} (panel c). The matrix and the fluid are $+1 : -1$ electrolytes, matrix concentration $c_0 = 0.5$ mol dm^{-3}, $L_B = 7.14$ Å, and quenching parameter $Q = 1.2$. A similar figure but for a different set of parameters was previously presented in ref. 34.

The influence of the matrix concentration on the structure of the annealed electrolyte is shown in Fig. 4. Here, the screened potentials of the fluid ion–ion interaction, $q^{11}(r)$, are presented at $Q = 1.2$, and different values of the matrix concentration: $c_0 = 0.005$ mol dm^{-3} (dash-dotted line), 0.05 mol dm^{-3} (dotted line), 0.5 mol dm^{-3} (continuous line), and 5 mol dm^{-3} (dashed line). Fig. 4a applies to a single fluid concentration, $c_1 = 5 \times 10^{-5}$ mol dm^{-3}, while in Fig. 4b the $q^{11}(r)$ functions are presented for a constant ratio, $c_1/c_0 = 0.1$. As intuitively, as well as previously established, the higher the matrix concentration, the stronger is its influence. At low fluid concentrations, such as in Fig. 4a, already a moderate matrix concentration causes the $q^{11}_{++}(r)$ and $q^{11}_{+-}(r)$ functions to intersect. Note that at relatively low fluid to matrix concentration ratio the intersecting of the curves does not occur even at high concentration of the matrix particles (Fig. 4b).

The results presented in this subsection are interesting *per se* showing the sensitivity of the properties of an annealed electrolyte to the structure of the quenched media. The results can be considered as the replica version of the Debye-Hückel limiting law as valid for bulk electrolytes (in this work we refer to it as the Debye-Hückel-like level of the ROZ theory). The results are further used in

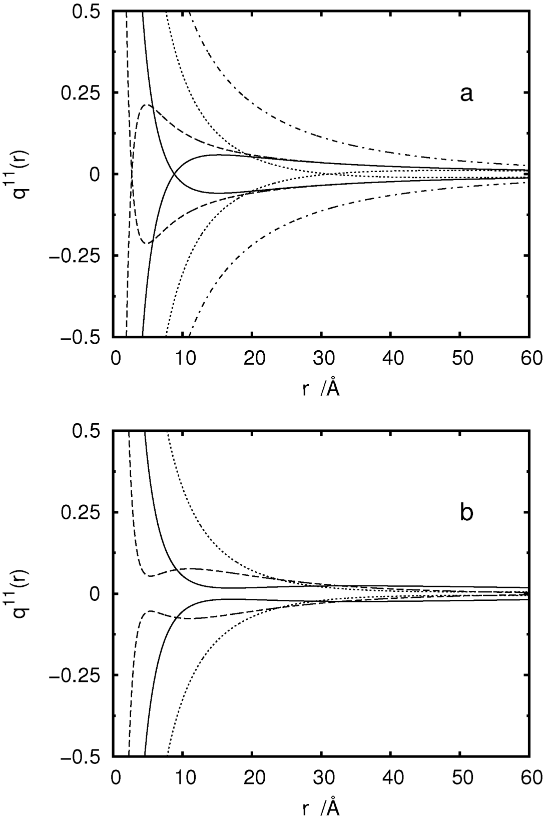

Fig. 4 The Debye-Hückel-like level of the ROZ theory. The screened potentials of the fluid ion–ion interaction, calculated using the eqn (18), at $Q = 1.2$ ($L_B = 7.14$ Å), and different values of the matrix concentration: $c_0 = 0.005$ mol dm^{-3} (dash-dotted line), 0.05 mol dm^{-3} (dotted line), 0.5 mol dm^{-3} (continuous line), and 5 mol dm^{-3} (dashed line). (a) $c_1 = 5 \times 10^{-5}$ mol dm^{-3}, (b) $c_1/c_0 = 0.1$.

a re-normalisation procedure of the ROZ equations to describe a more realistic primitive model electrolyte.

(b) Hypernetted-chain level of approach

An integral equation study of a screened Coulomb fluid in a disordered porous media was within the mean spherical approximation presented by Trokhymchuk *et al.*[76] The development of the re-normalisation procedure described in the previous subsection[34] made possible the integral equation study of unscreened Coulomb liquids. The ROZ study of Hribar *et al.*[35] of the primitive model electrolyte in the ionic matrix considered charge and size symmetric $+1:-1$ electrolyte in electroneutral $+1:-1$ ionic matrix. In this work two approximations, traditionally used to describe bulk electrolyte fluids (HNC and MSA) were used as closure conditions for the proper ROZ equations.[11] Both approximations were found to provide reasonably good agreement of thermodynamical and structural properties with the computer simulation results.[35] It is worth noting that the MSA closure is, setting the blocking part of the direct correlation function to zero,[3,7] just a special case of the Madden-Glandt approximation.[5]

Fig. 5 shows the comparison of the fluid-fluid pair distribution functions of the primitive model $+1:-1$ electrolyte in $+1:-1$ matrix newly obtained by three different methods: canonical Monte Carlo simulation (symbols), ROZ/HNC approximation (continuous lines), and Debye-Hückel-like approximation (dashed lines). The matrix concentration was $c_0 = 1.0$ mol dm^{-3}, while the fluid concentration, c_1, varied from 0.05 mol dm^{-3} (panel a), to 0.5 mol dm^{-3} (panel c), to capture different kinds of behaviour. In all cases, the quenching parameter $Q = 2.0$, $L_B = 7.14$ Å, and $\sigma_1 = \sigma_0 = 4.25$ Å. It can be seen from the comparison with the computer simulation results that the ROZ/HNC theory describes the structure of the annealed fluid very well, even at the extreme conditions where the fluid is under-screened (Fig. 5a), or over-screened (Fig. 5c). A similar figure but for a different set of parameters was previously presented in ref. 35. Similarly good agreement was obtained for structural properties of charge and size asymmetric electrolyte in a symmetric electroneutral matrices,[36] as well as in a asymmetric electrolyte[40] and hard-sphere matrices.[37]

It is worth mentioning again that at low fluid concentrations we observe disorder-induced attraction between similarly charged ions and concomitant repulsion between oppositely charged ions which is reflected in crossing of the fluid pair correlation functions (Fig. 5a). Another interesting observation is the increase of the $g^{11}_{+-}(r)$ contact value with the increasing fluid concentration, which is in contrast with the concentration dependence of the contact value in bulk electrolytes. All these results are consequences of the blocking effect of the matrix particles.

Thermodynamical properties, such as the excess internal energy and compressibility, calculated from the ROZ/HNC theory, as well as from the ROZ/MSA closure, were tested against computer simulations and show reasonably good agreement.[35–37] An important quantity describing the adsorption isotherms, however, is the chemical potential of the annealed fluid. The expression for the excess chemical potential valid within ROZ/HNC approximation was first introduced by Hribar *et al.*[37] and further established and tested against the grand canonical Monte Carlo (GCMC) simulations in ref. 40 and 41.

Fig. 6 shows the dependence of the reduced excess chemical potential, $\beta\mu^{ex}_{\pm}$, of the $+1:-1$ electrolyte on its concentration c_1 in the presence of the matrix

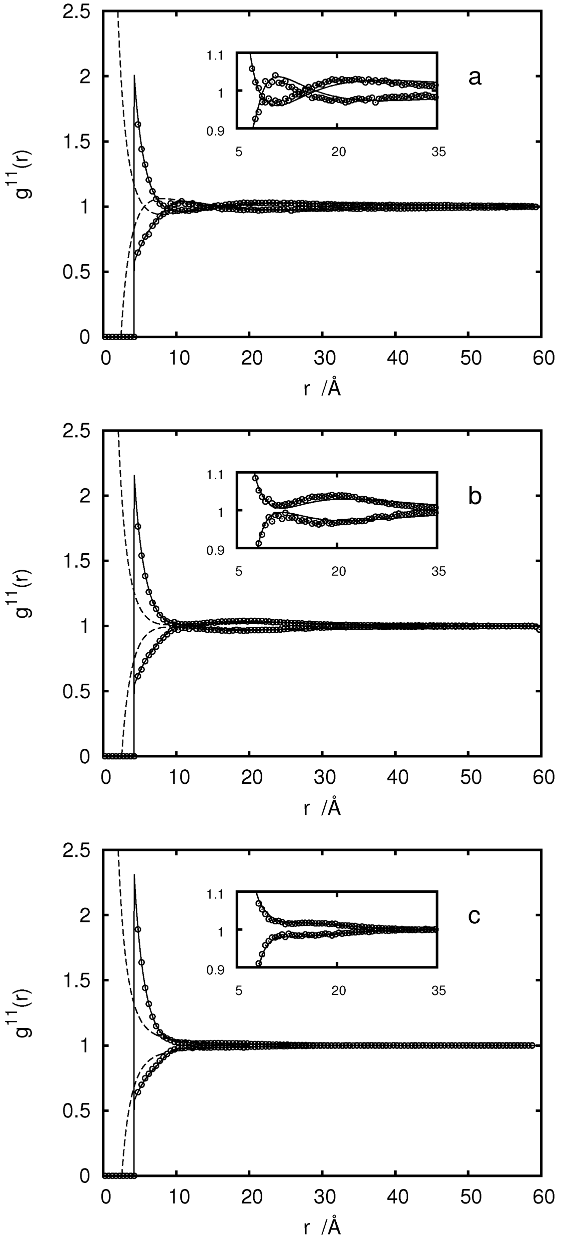

Fig. 5 The pair distribution functions, $g^{11}_{++}(r)$ and $g^{11}_{+-}(r)$, obtained with different methods: Monte Carlo simulation (symbols), ROZ/HNC approximation (continuous lines), and the Debye-Hückel-like approximation (dashed lines). Q = 2.0, L_B = 7.14 Å, $\sigma_1 = \sigma_0$ = 4.25 Å, c_0 = 1.0 mol dm^{-3}, c_1 = 0.05 mol dm^{-3} (panel a), 0.1 mol dm^{-3} (panel b), and 0.5 mol dm^{-3} (panel c).

(+1 : −1 electrolyte) particles with concentration c_0 = 0.4 mol dm^{-3} (continuous line) and in its absence (dotted line). For the comparison, the same quantity for a fully annealed mixture is also shown by a dashed line. Note that a similar figure but

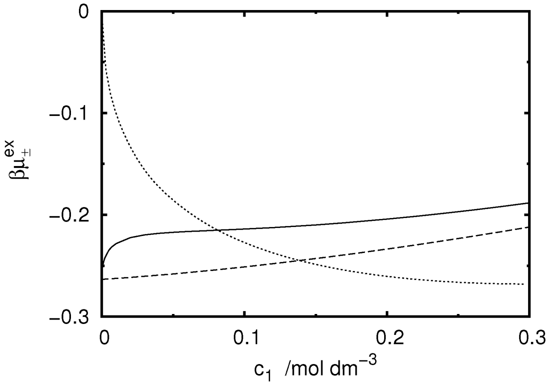

Fig. 6 The reduced excess chemical potential, $\beta\mu_{\pm}^{\mathrm{ex}}$, as a function of the annealed electrolyte concentration, c_1, for a symmetric $+1:-1$ electrolyte in a symmetric $+1:-1$ matrix with $c_0 = 0.4$ mol dm^{-3}. $Q = 1$, $L_B = 7.14$ Å, $\sigma_1 = \sigma_0 = 4.25$ Å. ROZ/HNC results are shown by continuous line, OZ/HNC results for a pure electrolyte are shown by a dotted line, and the results for a fully annealed mixture by a dashed line. A similar figure but for a different set of parameters was previously presented in ref. 40.

for a different set of parameters was previously presented in ref. 40. The reduced excess chemical potential of the adsorbed electrolyte differs substantially from the values obtained for a bulk electrolyte under the same conditions. At low fluid concentrations, the excess chemical potential, and with it the total chemical potential, is lower than that of a bulk fluid of the same concentration, causing an adsorption of the electrolyte in the matrix, while the opposite is true at larger fluid concentration, where the electrolyte gets "excluded" from the matrix.[40]

At infinite dilution, where the excess chemical potential of the fluid particles in a matrix reflects the affinity of the fluid species to matrix obstacles,[44,77] the values would approach those of a fully annealed fluid,[41] as expected for the case where $\varepsilon_0 T_0 = \varepsilon T$ ($Q = 1$), see Fig. 6.[27]

Fig. 7a shows the dependence of the reduced excess chemical potential of the annealed $+1:-1$ size symmetric electrolyte as a function of the square root of its concentration for different matrix concentrations at $Q = 1$: $c_0 = 0.2$ mol dm^{-3} (continuous line), 0.425 mol dm^{-3} (dashed line), and 1.0 mol dm^{-3} (dotted line). The lines show the results obtained using the ROZ/HNC theory, while the symbols show the results of GCMC calculations and were taken from ref. 41. A similar figure was first presented in ref. 41. The agreement between the results obtained by the two methods is excellent. The values of the chemical potential of the annealed fluid increase with the increasing matrix concentration in the whole concentration range studied here, which is a manifestation of the interaction between the matrix and the fluid particles.[44] At higher matrix concentrations, the matrix ions are better screened mutually and consequently electrostatic effect of the matrix on the annealed fluid is smaller. This effect is prevailing at low fluid concentrations. At higher fluid concentration, the "excluded volume" effect becomes more pronounced.[44]

It is worth mentioning that the adsorption of electrolyte mixtures of two annealed electrolytes with a common anion was studied using the the ROZ/HNC theory[39] and GCMC simulation technique.[78] Again, the agreement between the two approaches was very good. Depending on the properties (size, charge) of the cations, the preferential adsorption of one electrolyte over the other was observed.[39,78]

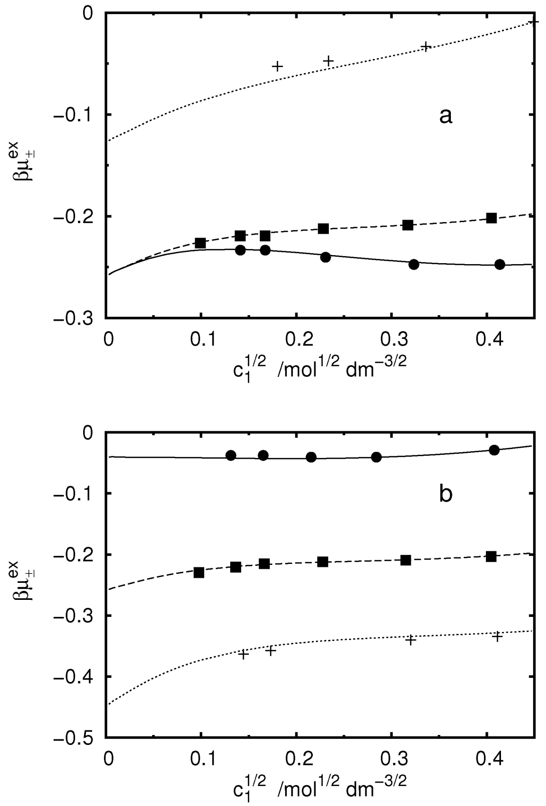

Fig. 7 The reduced excess chemical potential, $\beta\mu_{\pm}^{ex}$, as a function of the annealed electrolyte concentration, $c_1^{1/2}$, for a symmetric $+1:-1$ electrolyte in a symmetric $+1:-1$ matrix ($\sigma_1 = \sigma_0 = 4.25$ Å) at 298.15 K ($L_{B,0} = 7.14$ Å). ROZ/HNC results are shown by lines, and GCMC results (taken from ref. 41) are shown by symbols. (a) $Q = 1$, $c_0 = 0.2$ mol dm^{-3} (continuous line), 0.425 mol dm^{-3} (dashed line), and 1.0 mol dm^{-3} (dotted line). (b) $c_0 = 0.425$ mol dm^{-3}, $Q = 0.7$ (continuous line), 1.0 (dashed line), and 1.2 (dotted line). A similar figure was originally presented in ref. 41.

In the examples shown so far, the adsorption was studied at a single, (room) temperature. The influence of the conditions at which the adsorption takes place (temperature, solvent properties) were systematically explored in ref. 44. In this work[44] most of the calculations apply to the matrix formed at $T_0 = 298.15$ K with its dielectric constant being $\varepsilon_0 = 78.54$ ($L_{B,0} = e^2/4\pi\varepsilon'\varepsilon_0 k_B T_0 = 7.14$ Å). The properties of the annealed electrolyte were examined for a set of T and ε values. Note that the two parameters, T and ε, can be combined into one. For simplicity of presentation, ε was chosen to be equal to ε_0 in all the cases so the strength of the interaction between all ionic species was ascribed solely to the values of T.

Fig. 7b is showing the reduced excess chemical potential of the annealed $+1:-1$ electrolyte, adsorbed in the $+1:-1$ matrix prepared at 298.15 K, varying the conditions of observation. The ROZ/HNC results for $Q = 0.7$ ($L_B = 4.998$ Å) are shown by a continuous line, the results for $Q = 1.0$ ($L_B = 7.14$ Å) by a dashed line, and the results for $Q = 1.2$ ($L_B = 8.568$ Å) by a dotted line. The symbols represent the GCMC results taken from ref. 41. Similar figure was previously shown in ref. 41.

As expected, the reduced excess chemical potential of the annealed fluid decreases with decreasing the temperature or dielectric constant of the fluid, *e.g.*, with the increasing L_B.

In the cases where the fluid-fluid, as well as the fluid-matrix, interaction is stronger than the matrix-matrix one ($Q > 1$), an annealed ion will, on average, find itself in configurations such that an opposite charge exceeds its own charge. As a consequence, the competition between adsorption of the fluid ions on the matrix particles and the screened interactions between annealed ions leads to the rather complex behaviour of adsorption isotherms.[44]

The screening effect of the matrix on the behaviour of the adsorbed fluid can be seen also from the isothermal compressibility of the annealed fluid. Fig. 8 shows the reduced isothermal compressibility (*cf.* eqn (22)) of a model LiCl ($\sigma_+^1 = 5.43$ Å and $\sigma_-^1 = 3.62$ Å)[44] at different temperatures of observation in the absence (dotted lines), as well as in the presence of a $+1 : -1$ symmetric matrix ($\sigma_0 = 4.25$ Å) at $c_0 = 0.1$ mol dm^{-3} (continuous lines). All the results were obtained using the OZ or ROZ theory in the HNC approximation. The data for ROZ/HNC at T equal to 40 K were taken from ref. 44. A similar figure was previously presented in ref. 44. While the compressibility of the bulk electrolyte increases with the increasing concentration, the compressibility of the same electrolyte in the matrix first decreases and starts increasing only at intermediate concentrations. This indicates that the presence of the charged obstacles in the systems (matrix ions) strongly suppresses the concentration fluctuations in partly-quenched systems. Note that the reduced isothermal compressibility is shown as a function of the mean activity of the annealed electrolyte, $a_\pm$, defined as: $\ln a_\pm = \beta\mu_\pm^{ex} + \ln(c_1/1 \text{ mol dm}^{-3})$.

It is further seen that some of the lines describing the compressibility of the bulk electrolyte (dotted lines) at different temperatures are not complete. The reason for this is that at low temperatures and/or low concentrations the convergence problems are encountered using the HNC closure. On the other hand, for an electrolyte in the matrix convergent results can be obtained for much more stringent conditions.[44] It was suggested that the matrix phase, depending on its concentration, "stabilises" the

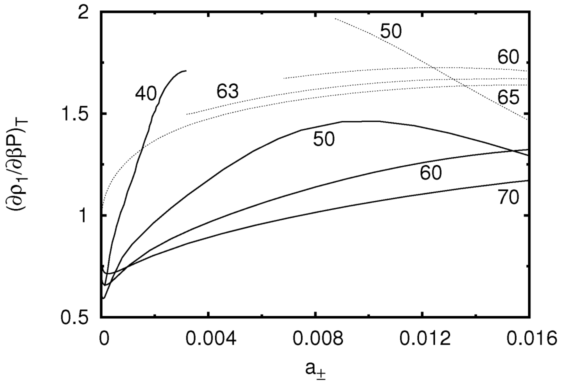

Fig. 8 The reduced isothermal compressibility (*cf.* eqn (22)) for a model LiCl at various temperatures of observation, T (as indicated in the figure), as a function of the mean activity, $a_\pm$. The dotted lines are calculated for the bulk electrolyte, and the continuous lines for the LiCl ($\sigma_+^1 = 5.43$ Å and $\sigma_-^1 = 3.62$ Å) in $+1 : -1$ electrolyte matrix with $c_0 = 0.1$ mol dm^{-3}, $T_0 = 298.15$ K, $\sigma_0 = 4.25$ Å (data for 40 K are taken from ref. 44). For the definition of the temperature consult the original paper.[44] A similar figure was originally presented in ref. 44.

adsorbed fluid: it inhibits the cation–anion pair formation, which appears to be overestimated by the OZ/HNC theory.[44]

(c) Templated systems

The microstructure of the matrix (not only the porosity but also the size and distribution of the micropores) is an important parameter dictating the adsorption of annealed fluids. It is reflected in the affinity of the fluid species to matrix obstacles and can be expressed as the reduced excess chemical potential of infinitely diluted fluid particles, $\beta\mu_{\pm}^{\mathrm{ex},1}$, in a matrix of concentration c_0, usually given in the form[44,77]

$$\exp[-\beta\mu_{\pm}^{\mathrm{ex},1}(c_1 = 0, c_0)] \tag{27}$$

It was shown, first by Van Tassel and Zhang,[46,47,79] that apart from temperature and dielectric constant, the quenched media structure can be influenced also by the template particles that are removed after the quench. The authors[46,47,79] extended the replica formalism to microporous non-ionic material treated by a template (denoted by the subscript $0'$).

The equations for an electrolyte in a hard sphere matrix templated by hard spheres were first presented by Dominguez *et al.*[45] and read

$$\begin{aligned} h_{i0}^{10} - c_{i0}^{10} &= c_{i0}^{10} \otimes \rho^0 h_{00}^{00} + c_{i0'}^{10'} \otimes \rho^{0'} h_{0'0}^{0'0} + c_{ii}^{11} \otimes \rho_i^1 h_{i0}^{10} \\ &\quad + c_{ij}^{11} \otimes \rho_j^1 h_{j0}^{10} - c_{ii}^{12} \otimes \rho_i^1 h_{i0}^{10} - c_{ij}^{12} \otimes \rho_j^1 h_{j0}^{10} \\ h_{i0'}^{10'} - c_{i0'}^{10'} &= c_{i0}^{10} \otimes \rho^0 h_{00'}^{00'} + c_{i0'}^{10'} \otimes \rho^{0'} h_{0'0'}^{0'0'} + c_{ii}^{11} \otimes \rho_i^1 h_{i0'}^{10'} \\ &\quad + c_{ij}^{11} \otimes \rho_j^1 h_{j0'}^{10'} - c_{ii}^{12} \otimes \rho_i^1 h_{i0'}^{10'} - c_{ij}^{12} \otimes \rho_j^1 h_{j0'}^{10'} \\ h_{ij}^{11} - c_{ij}^{11} &= c_{i0}^{10} \otimes \rho^0 h_{0j}^{01} + c_{i0'}^{10'} \otimes \rho^{0'} h_{0'j}^{0'1} + c_{ii}^{11} \otimes \rho_i^1 h_{ij}^{11} \\ &\quad + c_{ij}^{11} \otimes \rho_j^1 h_{jj}^{11} - c_{ii}^{12} \otimes \rho_i^1 h_{ij}^{21} - c_{ij}^{12} \otimes \rho_j^1 h_{jj}^{21} \\ h_{ij}^{12} - c_{ij}^{12} &= c_{i0}^{10} \otimes \rho^0 h_{0j}^{01} + c_{i0'}^{10'} \otimes \rho^{0'} h_{0'j}^{0'1} + c_{ii}^{11} \otimes \rho_i^1 h_{ij}^{12} \\ &\quad + c_{ij}^{11} \otimes \rho_j^1 h_{jj}^{12} + c_{ii}^{12} \otimes \rho_i^1 h_{ij}^{11} + c_{ij}^{12} \otimes \rho_j^1 h_{jj}^{11} \\ &\quad - 2c_{ii}^{12} \otimes \rho_i^1 h_{ij}^{21} - 2c_{ij}^{12} \otimes \rho_j^1 h_{jj}^{21} \end{aligned} \tag{28}$$

The dependence of the correlation functions on r was for clarity of presentation omitted. The set of eqn (28) was re-normalised and solved in the HNC approximation. Note that the presence of the templated particles does not change the form of the $q_{ij}^{mn}(r)$ functions given by eqn (18).[45,52] Within this same approximation, the equation for the excess chemical potential reads[45]

$$\begin{aligned} \beta\mu_{i,1}^{\mathrm{ex}} &= -\rho^0 \mathbf{c}_{\mathbf{(s)i0}}^{\mathbf{10}}(\mathbf{0}) - \rho^{0'} \mathbf{c}_{\mathbf{(s)i0'}}^{\mathbf{10'}}(\mathbf{0}) - \sum_{j=+,-} \rho_j^1 [\mathbf{c}_{\mathbf{(s)ij}}^{\mathbf{11}}(\mathbf{0}) - \mathbf{c}_{\mathbf{(s)ij}}^{\mathbf{12}}(\mathbf{0})] \\ &\quad + \frac{1}{2}\rho^0 \int h_{i0}^{10}(r)[h_{i0}^{10}(r) - c_{i0}^{10}(r)]\mathrm{d}\mathbf{r} + \frac{1}{2}\rho^{0'} \int h_{i0'}^{10'}(r)[h_{i0'}^{10'}(r) - c_{i0'}^{10'}(r)]\mathrm{d}\mathbf{r} \\ &\quad + \frac{1}{2}\sum_{j=+,-} \rho_j^1 \int \{h_{ij}^{11}(r)[h_{ij}^{11}(r) - c_{ij}^{11}(r)] - h_{ij}^{12}(r)[h_{ij}^{12}(r) - c_{ij}^{12}(r)]\}\mathrm{d}\mathbf{r} \end{aligned} \tag{29}$$

Fig. 9 shows the adsorption isotherms for a model LiCl ($\sigma_+^1 = 5.43$ Å and $\sigma_-^1 = 3.62$ Å) at 298.15 K ($L_B = 7.14$ Å) in a hard sphere matrix as a function of the mean activity of the annealed electrolyte, $a_\pm$. $\sigma_0 = 5.0$ Å and $\sigma_{0'} = 6.0$ Å. The continuous lines apply to untemplated, and symbols (taken from ref. 45, connected by dashed lines) to templated matrix ($c_{0'} = 1.0$ mol dm^{-3}). The top two curves apply

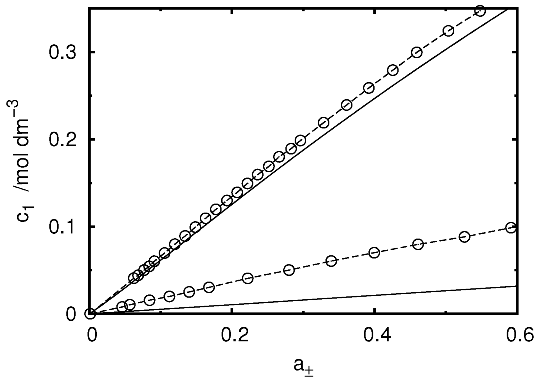

Fig. 9 The adsorption isotherms for a model LiCl ($\sigma^1_+ = 5.43$ Å and $\sigma^1_- = 3.62$ Å) in a hard sphere matrix ($\sigma_0 = 5$ Å) as a function of the mean activity, $a_\pm$. The continuous lines apply to the untemplated and the symbols (taken from ref. 45 and connected by dashed lines) to templated matrix ($\sigma_{0'} = 6$ Å, $c_{0'} = 1.0$ mol dm^{-3}). The top two curves apply to $c_0 =$ 2 mol dm^{-3}, and the bottom ones to $c_0 = 6$ mol dm^{-3}. A similar figure was originally presented in ref. 45. Note a misprint in the original ref. 45 where c_0 values are stated to be twice too small. The correct values are given here.

to $c_0 = 2$ mol dm^{-3} and the bottom two to $c_0 = 6$ mol dm^{-3}. Similar figure was previously published in ref. 45.

For both matrix concentrations, the adsorption in templated matrices is higher than in the untemplated.[45] The effect is more pronounced at higher matrix concentrations and can be explained as follows: the presence of template particles causes less uniform distribution of the obstacles. After the removal of the template, the matrix has, on one hand, dense domains where it is difficult to insert a pair of ions and on the other hand "microcavities" where such an insertion is facilitated and where ions have fewer unfavourable contacts with matrix particles.[45] As a consequence, the adsorption is enhanced in templated matrices.

(d) Matrices with non-zero net charge

An important example of templated matrices that requires special attention are matrices with non-zero net charge. The matrix in this case is prepared by equilibrating an electrolyte solution at temperature T_0, however, after the quench, only anions are "frozen" in their positions, while cations are allowed to equilibrate[52,80] (or *vice versa*). The ROZ equations, treating the matrix cations as template particles in the matrix (anions) are given in ref. 52 and are in principle the same as eqn (28), the particles "0" being the the matrix anions, while the index "0′" denotes the matrix cations. Again, of special interest are the adsorption isotherms that are determined by the activity of the electrolyte in the matrix. The equation for the reduced excess chemical potential is given by eqn (29).[45,52]

Lukšič *et al.*[52] showed important qualitative differences in the adsorption in charged matrices compared to electroneutral ones. One such comparison is given in Fig. 10 which shows the relation between the concentration of the adsorbed +1 : −1 electrolyte ($\sigma_1 = 4.25$ Å), c^1_-, and its mean activity, $a^1_\pm$, for (a) $c_0 = 0.5$ mol dm^{-3} and (b) $c_0 = 1.0$ mol dm^{-3}. $L_B = L_{B,0} = 7.14$ Å, $\sigma^0_- = \sigma^{0'}_+ = 4.25$ Å. The mean activity of the annealed charge symmetric electrolyte considered here is defined as $a^1_\pm = (c^1_+ c^1_- \gamma^2_\pm)^{1/2}$, where $\ln\gamma^1_\pm = \beta\mu^{\rm ex}_\pm$. The continuous lines represent the

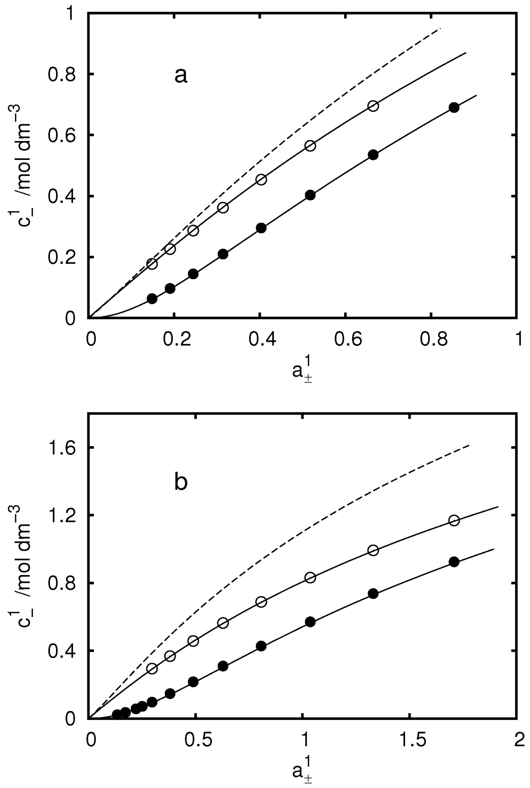

Fig. 10 The dependence of the adsorbed $+1:-1$ electrolyte concentration c_-^1, on its mean activity, $a_\pm^1$, for two different matrix concentrations: (a) $c_0 = 0.5$ mol dm^{-3} and (b) $c_0 = 1.0$ mol dm^{-3}. $L_B = L_{B,0} = 7.14$ Å, $\sigma_1 = \sigma_-^0 = \sigma_+^{0'} = 4.25$ Å, $z_-^0 = -1$ and, $z_+^{0'} = +1$. The continuous lines represent the ROZ/HNC results and the symbols correspond to GCMC results. The dashed line shows the OZ/HNC results for the bulk electrolyte, the middle line shows the results for the electroneutral matrix (empty symbols), and the bottom line shows the results for the charged matrix (full symbols). Reprinted with permission from ref. 52. Copyright 2007 American Chemical Society.

ROZ/HNC results and the symbols correspond to GCMC results. The dashed line shows the OZ/HNC results for the bulk electrolyte, the middle line shows the results for the electroneutral matrix (empty symbols), and the bottom line shows the results for the charged matrix (full symbols).[52]

There are qualitative differences in the mechanism of the adsorption for the two cases presented in Fig. 10. In the case of the electroneutral matrix, the matrix is represented by some equilibrium distribution of positive and negative ions frozen in their positions. The spatial distribution of fixed positive and negative charges that is determined by the pre-quenching conditions (temperature, dielectric constant, concentration c_0) influences the adsorption of the electrolyte in such a material. For example, if the matrix contains a large fraction of the +,− ion-pairs (only dipoles in an extreme situation), then the adsorption power of such a matrix would be considerably different from the one containing little or no ion pairs.[81] The invading electrolyte cations and anions are, namely, attracted by the matrix charges, each of them to the opposite charge. If these charges are well separated the adsorption is stronger; in the case of a dipolar fluid (small charge separation), it is much weaker. There is, however, always an "excluded volume" effect to be considered. The latter works against the adsorption and gains its importance for dense matrices.[37]

In the case of charged matrices, the matrix possesses net (negative in the case presented here) fixed charge,[52] which attracts electrolyte cations and repels anions. The primary parameter in such a case is the charge density (depending on concentration and charge of the obstacles) of the matrix. Porous material, together with an invading electrolyte, forms an electroneutral system. The resulting adsorption (or desorption) of the electrolyte depends most notably on the matrix charge and dielectric constant of the solvent, as also on the concentration and composition of the invading electrolyte. In most cases, the result is the electrolyte rejection, which can be, by the mean-field type of arguments, explained as follows: the mean electrostatic potential in the matrix containing net negative charge is negative which makes it more difficult for the negative ions, and because of the electroneutrality condition their positive counterparts, to enter the matrix. These arguments which derive from the classical electrical double-layer theory[82] are only approximately correct because they ignore the correlation between the invading ions and fixed charges. The correlation effects, not taken into account by the classical Poisson-Boltzmann's approach, are especially strong for multivalent counterions if present in solution. It was shown theoretically, and to a certain degree also documented by experiment, that the effect may ultimately change the sign of the Donnan exclusion coefficient.[83,84]

A similar study, but for a two-dimensional positively charged matrix formed from an asymmetric electrolyte, was recently published by Lomba and Weiss.[85] The ROZ/HNC theory was tested against Monte Carlo computer simulation for structural and thermodynamical properties and good agreement was obtained. Interesting results, not presented before, are the results for the individual chemical potentials of the annealed ions that show strong dependence on the matrix structure.

(e) Other potentials/systems in external field

Up to here, we were concerned with simple models of electrolytes in partly-quenched systems, treating particles (ions) as charged hard spheres. A successful description of realistic molecular liquids of various complexity is feasible within the so-called reference interaction site model (RISM) in the replica formalism.[86] The theory, pioneered by Chandler and Andersen,[87] is an orientational reduction of the molecular OZ integral equation and can handle the description of the solution including polar and nonpolar polyatomic molecules as well as polyatomic ions and various chemical specificities such as hydrogen bonding.[88] Hirata and co-workers[49,51] have extended the RISM theory to polar liquids and ions in molecular polar solvent, and successfully extended replica RISM equations for describing quenched disorder in realistic molecular systems with polar and charged species. As a first example, the authors have studied the extended simple point charge model water adsorbed into a quenched microporous material of molecular species that also contained charges. To avoid divergence, Kovalenko and Hirata utilised the partly linearised hypernetted-chain closure for the site-site correlations

$$g^{ij}_{\alpha\gamma}(r) = \begin{cases} \exp[d^{ij}_{\alpha\gamma}(r)], & d^{ij}_{\alpha\gamma}(r) \leq 0 \\ 1 + d^{ij}_{\alpha\gamma}(r), & d^{ij}_{\alpha\gamma}(r) > 0 \end{cases} \tag{30}$$

$$d^{ij}_{\alpha\gamma}(r) = -\beta u^{ij}_{\alpha\gamma}(r) + h^{ij}_{\alpha\gamma}(r) - c^{ij}_{\alpha\gamma}(r)$$

where $g^{ij}_{\alpha\gamma}(r) = h^{ij}_{\alpha\gamma}(r) + 1$ are the site-site distribution functions, and $u^{ij}_{\alpha\gamma}(r)$ are the site-site interaction potentials. This closure combines the HNC approximation for density depletion regions of $h^{ij}_{\alpha\gamma}(r) < 0$ and MSA for enrichment regions of $h^{ij}_{\alpha\gamma}(r) > 0$. The main conclusions of the work mentioned above (water confined in matrices of quenched network of interconnected branched chains with or without grafted activating polar groups) are that the matrix confinement increases the compressibility of ambient water and that it rises its excess chemical potential. Hydrogen bonding in water and for water molecules adsorbed at activating carboxylic groups is considerably enhanced by the presence of the matrix phase. With respect to this, we would like also to mention the paper of Urbič *et al.*[48] who studied a very simple two-dimensional model of water in the presence of Lennard-Jones obstacles utilising an associative ROZ theory. Although the model is much simpler than the model of Kovalenko and Hirata,[49] the authors came to identical conclusions. Mentioned works are relevant for studying water inside biological cells, which are characterised by a high degree of molecular crowding from organelles and high concentration of biomolecules.

Replica RISM theory was recently used to investigate the structure of electrolyte solutions confined in carbonised polyvinylidene chloride nanoporous material.[51] The work is important in the light of electric energy storage devices research since the model mimics the electric double layer capacitor. The structure of the electrolyte solution sorbed in carbon nanopores exhibits substantial changes in comparison to the (unperturbed) bulk solution. Due to the reduced density of the sorbed solution, hydrogen bond network of water molecules is different from that in the bulk, and water molecules make small clusters coexisting with regions of water vapour. The ion–water interaction is enhanced due to reduced density of the solution. Cations are distributed more or less evenly over the pore space, while anions can access the carbon surface and stay in direct contact with the surface. Differences in the behaviour of cations and anions are explained with their hydration nature.

Another interesting field of research are solutions of polyelectrolytes. For instance, Bratko and Chakraborty[21] have considered a linear polyion embedded in a disordered medium with quenched fluctuations in the density of ionic sites that comprise the disorder. They have utilised the Monte Carlo simulations and the Feyman-Bogoliubov variational method to conclude that the charge-density fluctuations in the system cause the effective interaction between equally charged beads to displays a minimum at characteristic distance $r_{\min}$ and that the interaction is attractive at large separations. This feature is explained by the attraction of the beads to the same potential walls created by the accumulation of oppositely charged ionic sites of the quenched disorder. The polyion tends to reduce its Coulomb energy by assuming configurations favouring optimal bead to bead distances, $r_{\min}$.

With respect to polyelectrolyte solutions, recent works of Fleck and Netz[89] and Podgornik *et al.*[90–92] need to be mentioned. These authors have investigated the effect of quenched surface charge disorder of the macroion on the electrostatic interactions between charged surfaces surrounded by the mobile neutralising counterions. In many cases of biological importance (DNA microarrays, surfactant-coated surfaces, random polyelectrolytes and polyampholites *etc.*) the charge patterns along macromolecular complex surface are inhomogeneous and exhibit a highly disordered spatial distribution. Since interactions between macroions are essential for maintaining their complex structure and function such research is highly desirable. Poisson-Boltzmann approach treating charge on the surfaces of macroions as homogeneous and constant cannot explain the unexpected and counter-intuitive collapse of highly charged polyelectrolytes (*e.g.*, DNA) in the presence of polyvalent counterions. Utilising field-theoretic and replica methods the authors showed that in the case of the presence of neutralising counterions, the quenched disordered distribution of macroion's surface charges induces an additive interaction in the strong-coupling limit even if the mean charge of the macroions is zero. For small distances from the macroion's surface a pronounced enhancement of the counterion density was found, caused by the coupling between surface ion disorder and counterions. Podgornik *et al.*[90–92] investigated also the interesting effects connected with the partial annealing of the disorder and found that partial annealing of the surface charges leads to additional attractive interactions between the surfaces and may even result in a global attractive instability of the system.

Membrane equilibria can also be studied in the framework of partly-quenched systems with directional dependent potentials. Models of partly-quenched systems with permeable interfaces are of considerable interest as they represent simple prototypes of membrane partitioning. Bryk *et al.*[93] used a density functional approach to study phase behaviour of a Lennard-Jones fluid in a system with slit-like pores separated by semipermeable walls while Boda and co-workers[94] studied the selective partitioning of two restricted primitive electrolytes across the membrane, permeable to only one electrolyte, using the Monte Carlo simulations and density functional theory. A review of the density functional theory (DFT) for quenched-annealed fluid mixtures is given by Schmidt in ref. 95, 96. The author, however, deals only with uncharged systems. DFT for systems containing ions is, *e.g.*, given in ref. 94 and 90–92.

Bracamontes *et al.*[97] used grand canonical Monte Carlo simulation and ROZ integral equation theory to study a hard sphere fluid in an array of permeable obstacles. The difference from matrices described in previous subsections is in the direction-dependent potential between the annealed and the matrix species. The authors used the following potential

$$U^{10}(r) = 4\varepsilon^{10}\,\frac{U_0 - (U_0 + \varepsilon^{10})\left(\frac{\sigma_0/2 - r}{w}\right)^{6}}{4\varepsilon^{10} + (U_0 + \varepsilon^{10})\left(\frac{\sigma_0/2 - r}{w}\right)^{12}} \qquad (31)$$

to model the membrane, where ε^{10} denotes the depth of the attractive part of the potential, U_0 is the height of the barrier and w is the half-width of the barrier. If ε^{10} is small, the potential becomes almost entirely repulsive. For large values of ε^{10} attraction between fluid particles on both surfaces of the model membrane barrier exposed to the interior of each matrix cavity and to the external porous space is obtained. Preliminary results on partitioning of the simple ions through such membrane were obtained by one of us using machine calculations. Parameters $\varepsilon^{10} = 0.5\ k_BT$ and $w = 2$ Å were set equal for anions and cations of the restricted primitive $+1 : -1$ electrolyte (the diameters of ions were 4.25 Å), while the heights of the barriers were $U_0^+ = 8\ k_BT$ and $U_0^- = 2\ k_BT$ for cations and anions, respectively. It was established that both kinds of ions crowded at the inner and outer surface of the cell membrane, the concentration of positive ions being slightly smaller than the negative ones. This effect became more pronounced with an increasing concentration of the electrolyte. At high electrolyte concentrations (0.02 mol dm^{-3}) the consequence of smaller penetration of positive ions was noticed also outside the cell, where there were more positive than negative ions in the contact with the cell. Within the membrane, there were no positive ions and a very small concentration of negative ions, irrespective of the concentration of the annealed electrolyte. Studies of matrices formed by permeable obstacles (vesicles) selective to one ionic species are of interest for all applications that require the removal of a particular ionic species, for example heavy metals or radionuclides.

At the end of this subsection, we wish to mention the work of Pizio and co-workers[98,99] who developed the inhomogeneous replica Ornstein-Zernike equations to study fluid adsorbed in slit-like pore filled with a quenched disordered hard sphere fluid. As already stressed, such situations are important in gel-exclusion chromatography techniques, extraction from porous rocks, study of fluids adsorbed in clays with quenched disordered pillar *etc*. To our best knowledge, no reports on inhomogeneous ROZ for ionic systems have been published so far.

(f) Dynamical properties

In vitro construction of artificial tissues from human stem cells, biodegradation of organic contaminants by microbial biofilms, the delivery of chemotherapeutical agents to malignant tumors, and storage of radioactive ions in nuclear waste are just few of the processes where dynamical phenomena play a crucial role.[100–103] The first theoretical work considering the ion motion in charged disordered materials were performed by Chakraborty *et al.*,[22] and Deem and Chandler.[24] They used approximate theories to study the effect of the matrix disorder on the diffusion of the ions. They showed that the diffusion coefficient decreases with the disorder strength of the porous media and at a certain value abruptly goes to zero.

Recently, Jardat *et al.* presented the Brownian dynamics study of the self-diffusion coefficients of ions of the charge- and size-symmetric $+1 : -1$ electrolyte in the presence of ionic disordered electroneutral matrix.[58] In this study, the ions interacted with each other through a "soft" Coulomb potential.[58] During the process of the simulation, the trajectories of the annealed particles were computed, and the self-diffusion coefficient, D, was obtained from the auto-correlation function of the force using the expression[58]

$$D = D^0 - \frac{1}{3}\int_0^{\infty} (\beta D^0)^2 \langle F(t_0 + t)F(t_0)\rangle \mathrm{d}t \tag{32}$$

where $F(t_0)$ and $F(t_0 + t)$ are the forces on the particle at some arbitrary initial time t_0 and at some later time $t_0 + t$, respectively.

The study was concerned with the self-diffusion of the annealed ions, as measured by D/D^0, D^0 being the self-diffusion coefficient of ions at infinite dilution, *i.e.*, without any interactions. Since fluid and matrix were both represented as a charge and size symmetric electrolytes, $D_+ = D_- = D$.

Fig. 11 shows the self-diffusion coefficient, D, of ions divided by the value at infinite dilution, D^0, as obtained with the Brownian dynamics method.[58] Open squares denote the results for the annealed electrolyte of concentration c_1 in the matrix with $c_0 = 0.425$ mol dm^{-3}. The open circles denote the results for the mixture of identical $+1 : -1$ electrolytes with concentrations 0.425 mol dm^{-3} and c_1. The presence of obstacles reduces the value of the self-diffusion coefficient more than the presence of the mobile ions at the same total concentration. Although there are qualitative differences in concentration dependence of D/D^0 in both cases (in the bulk electrolyte D/D^0 decreases with increasing concentration, while it first increases and than decreases in the case of the matrix present), the difference between the two sets of results becomes smaller with the increasing electrolyte concentration c_1.

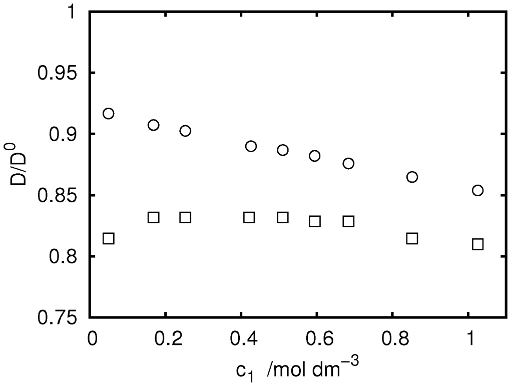

Fig. 11 Self-diffusion coefficient, D, of ions divided by the value at infinite dilution, D^0. Open squares denote the results for the annealed electrolyte of concentration c_1 in the matrix with $c_0 = 0.425$ mol dm^{-3}. The open circles denote the results for the mixture of identical $+1 : -1$ electrolytes with concentrations 0.425 mol dm^{-3} and c_1. From ref. 58—Reproduced by permission of The Royal Society of Chemistry.

In the last decade, molecular dynamics was vastly used to study the dynamics and transport in charged (not electroneutral) porous media,[104–108] mostly clays. The results of these studies confirm the generally admitted ideas that anions are repelled by the negatively charged external surface of clays, while on the contrary, the cations are attracted by the surface and may exchange with the natural inter-layer counterions.[106] It has been shown that the empirical partitioning coefficients between mobile and trapped ions can be evaluated from the microscopic dynamics of ions.[105] The latter is, depending on the fluid concentration, controlled by two different mechanisms. While at low concentration the Coulomb attraction between fluid and matrix particles increases the equilibrium concentration of the fluid in the matrix, the excluded volume effect dominates at high concentrations, reducing the amount of the ionic fluid entering the matrix.[108] These findings are consistent with the thermodynamical results[52] and can be explained with continuous solvent models. The exchange of cations in clays (ion-exchange process), however, was recently found to be driven by ‘‘hydrophobicity’’ and not by the affinity of ions for charged clay surface.[107]

Most of the theoretical investigations of dynamics of partly-quenched ionic systems described above, as well as the experimental results, apply to charged microporous materials with well defined geometry.[101] Very interesting, yet unpublished, results were obtained by Jardat *et al.*[59] for disordered non-electroneutral matrices. The authors focused on the self-diffusion coefficients of ions, D, in charged matrices.[59] Jardat and coworkers studied the behaviour of individual self-diffusion coefficients for coions (ions of the same charge sign as the matrix) and counterions (ions of the opposite charge sign than the matrix ions) in matrices made of -1, and -10 charges, respectively. In -1 matrices and at higher concentration of -10 matrices, the counterions become faster than the coions.[59] This result is in qualitative agreement with the predictions of the thermodynamical mean-field theory as described above, as well as with with recent coarse-grained simulations of Rotenberg *et al.* of effective diffusion coefficient of charged tracers in a charged porous media saturated by an electrolyte solutions.[61] The explanation was suggested that the counterions follow preferential pathways along the surfaces of the porous medium, while the coions have a bigger volume to explore and are therefore slower.[59] However, an unexpected and not yet completely understood results is that in matrices made of -10 charges at low matrix concentrations, the counterions are slowed down and coions become faster ($D_-/D_-^0 > D_+/D_+^0$).[59] It seems that the combined influence of the excluded volume and the electrostatic interaction causes a change in the mechanism of transport.

4. Conclusion and perspectives

In this contribution, we reviewed theoretical developments in the field of partly-quenched systems containing charges. We briefly discussed the methods used to investigate such systems, but laid more stress on the results setting guidelines for possible applications. Understanding the properties of ionic solutions trapped in the quenched environment is, as mentioned several times before, of great practical importance. For illustration: many porous materials, acting as membranes or retention barriers in various industrial, environmental, and biological processes, contain charges. This makes them—together with the invading electrolyte solution—good candidates to be examined by the replica methodology. The story, of course, does not end here; the replica theory can be applied to any system in which some degrees of freedom are quenched and the others are annealed. One such example is the study of DNA unzipping phase diagram.[109] Development of the replica methodology for more advanced models is desirable also from the perspective of ionic solvation. The water molecules buried inside a protein are often considered as an integral part of the protein structure. The rotation of these molecules is hindered in comparison with the rotational freedom of the bulk water; in principle they could be treated within the formalism used for partly-quenched systems. Further development of the replica methodology would need to be directed toward studies of more realistic matrices and interaction potentials. In this respect, we see a great potential of the integral equation approaches reviewed here. The ROZ theory provides results in good agreement with computer simulation and, in contrast to the latter, it does not require a detailed information on the matrix structure. The input data to the theory can in principle be provided through the experimentally obtained structure factor(s), what may eventually pave the path for theoretical investigations of more realistic systems.

There is a need for further development of theories for ionic and molecular systems based on the replica formalism. One direction is, for example, an extension of the theory to systems under the influence of an external field. The other is to treat the partly-quenched ionic systems in the framework of some kind of perturbation approach or, as it was done recently by Holovko and Dong for hard spheres,[110] within the "scaled particle" theory. Further, an interesting problem of the symmetry-breaking for the fluids within the charged material has not been solved yet. Some other challenging issues to be addresses in this field of science were pointed out by Sarkisov and van Tassel[86] in the concluding section of their review paper.

However, the role of computer simulations in investigating partly-quenched systems, molecular dynamics in particular, should not be overlooked. They are indispensable for studying ionic transport in systems with coupled solvent and charge flow in the vicinity of charged surfaces, causing the so-called electro-kinetic phenomena. These are of great practical importance in fields as diverse as micro-fluidics, colloid science and oil exploration.[101]

All in all, we believe that the partly-quenched systems containing charges will remain a vivid and important field of research also in the future.

References

1 O. Pizio and S. Sokołowski, *J. Phys. Studies*, 1998, **2**, 296.
2 M. L. Rosinberg, in *New Approaches to Problems in Liquid State Theory*, C. Caccamo, J. P. Hansen and G. Stell, ed. Kluwer, Dordrecht, 1999, pp. 245–278.
3 O. Pizio, in *Computational Methods in Surface and Colloid Science (Surfactant science series, vol. 89)*, M. Borowko, ed. Kluwer, Marcel Dekker, New York, 2000, pp. 293–345.
4 W. G. Madden, *J. Chem. Phys.*, 1992, **96**, 5422.
5 W. G. Madden and E. D. Glandt, *J. Stat. Phys.*, 1988, **51**, 537.
6 J. A. Given, *J. Chem. Phys.*, 1995, **102**, 2934.
7 J. A. Given and G. Stell, *J. Chem. Phys.*, 1992, **97**, 4573.
8 J. A. Given and G. Stell, *Physica A*, 1994, **209**, 495.
9 J. A. Given and G. Stell, in *Condensed Matter Theories (vol. 8)*, L. Blum and F. B. Malik, ed. Plenum, New York, 1993, pp. 395–410.
10 H. Tatlipinar, G. Pastore and M. P. Tosi, *Philos. Mag. Lett.*, 1993, **68**, 357.
11 E. Lomba, J. A. Given, G. Stell, J. J. Weis and D. Levesque, *Phys. Rev. E*, 1993, **48**, 233.
12 L. A. Fanti, E. D. Glandt and W. G. Madden, *J. Chem. Phys.*, 1990, **93**, 5945.
13 M. L. Rosinberg, G. Tarjus and G. Stell, *J. Chem. Phys.*, 1994, **100**, 5172.
14 A. Meroni, D. Levesque and J. J. Weis, *J. Chem. Phys.*, 1996, **105**, 1101.
15 R. D. Kaminsky and P. A. Monson, *J. Chem. Phys.*, 1991, **95**, 2936.
16 C. Vega, R. D. Kaminsky and P. A. Monson, *J. Chem. Phys.*, 1993, **99**, 3003.
17 D. M. Ford and E. D. Glandt, *J. Chem. Phys.*, 1994, **100**, 2392.
18 A. D. Trokhymchuk, O. Pizio, M. F. Holovko and S. Sokołowski, *J. Phys. Chem.*, 1996, **100**, 17004.
19 E. Kierlik, M. L. Rosinberg, G. Tarjus and P. A. Monson, *J. Chem. Phys.*, 1997, **106**, 264.
20 E. Pitard, M. L. Rosinberg, G. Stell and G. Tarjus, *Phys. Rev. Lett.*, 1995, **74**, 4361.
21 D. Bratko and A. K. Chakraborty, *Phys. Rev. E*, 1995, **51**, 5805.
22 A. K. Chakraborty, D. Bratko and D. Chandler, *J. Chem. Phys.*, 1994, **100**, 1528.
23 D. Wu, K. Hui and D. Chandler, *J. Chem. Phys.*, 1992, **96**, 835.
24 M. W. Deem and D. Chandler, *J. Stat. Phys.*, 1994, **76**, 911.
25 K. Leung and D. Chandler, *J. Chem. Phys.*, 1995, **102**, 1405.
26 P. A. Gordon and E. D. Glandt, *J. Chem. Phys.*, 1996, **105**, 4257.
27 D. Bratko and A. K. Chakraborty, *J. Chem. Phys.*, 1996, **104**, 7700.
28 M. Muthukumar, *J. Chem. Phys.*, 1989, **90**, 4594.
29 A. P. Y. Wong and M. H. W. Chan, *Phys. Rev. Lett.*, 1990, **65**, 2567.
30 B. J. Frisken and D. S. Cannell, *Phys. Rev. Lett.*, 1992, **96**, 632.
31 M. C. Goh, W. I. Goldburg and C. M. Knobler, *Phys. Rev. Lett.*, 1987, **58**, 1008.
32 J. V. Maher, W. I. Goldburg, D. W. Pohl and M. Lanz, *Phys. Rev. Lett.*, 1984, **53**, 60.
33 A. P. Y. Wong, S. B. Kim, W. I. Goldburg and M. H. W. Chan, *Phys. Rev. Lett.*, 1993, **79**, 954.
34 B. Hribar, O. Pizio, A. Trokhymchuk and V. Vlachy, *J. Chem. Phys.*, 1997, **107**, 6335.
35 B. Hribar, O. Pizio, A. Trokhymchuk and V. Vlachy, *J. Chem. Phys.*, 1998, **108**, 2480.
36 B. Hribar, V. Vlachy, A. Trokhymchuk and O. Pizio, *J. Phys. Chem. B*, 1999, **103**, 5361.
37 B. Hribar, V. Vlachy and O. Pizio, *J. Phys. Chem. B*, 2000, **104**, 4479.
38 V. Vlachy, T. Ichiye and A. D. J. Haymet, *J. Am. Chem. Soc.*, 1991, **133**, 1077.
39 M. Lukšič, G. Trefalt and B. Hribar-Lee, *Condens. Matter Phys.*, 2009, **12**, 717.
40 B. Hribar, V. Vlachy and O. Pizio, *J. Phys. Chem. B*, 2001, **105**, 4727.
41 B. Hribar, V. Vlachy and O. Pizio, *Molec. Phys.*, 2002, **100**, 3093.
42 L. Belloni, *J. Chem. Phys.*, 1985, **99**, 43.
43 L. Belloni, *J. Chem. Phys.*, 1988, **88**, 5143.
44 V. Vlachy, H. Dominguez and O. Pizio, *J. Phys. Chem. B*, 2004, **108**, 1046.
45 H. Dominguez, B. Hribar, V. Vlachy and O. Pizio, *Physica A*, 2003, **324**, 469.
46 L. Zhang and P. R. Van Tassel, *Mol. Phys.*, 2000, **98**, 1251.
47 L. Zhang and P. R. Van Tassel, *J. Chem. Phys.*, 2000, **112**, 3006.
48 T. Urbič, V. Vlachy, O. Pizio and K. A. Dill, *J. Molec. Liquids*, 2004, **112**, 71.
49 A. Kovalenko and F. Hirata, *J. Chem. Phys.*, 2001, **115**, 8620.
50 A. Tanimura, A. Kovalenko and F. Hirata, *Chem. Phys. Letters*, 2003, **378**, 638.
51 A. Tanimura, A. Kovalenko and F. Hirata, *Langmuir*, 2007, **23**, 1507.
52 M. Lukšič, B. Hribar-Lee and V. Vlachy, *J. Phys. Chem. B*, 2007, **111**, 5966.
53 A. R. Mehrabi and M. Sahimi, *Phys. Rev. Lett.*, 1999, **82**, 735.

54 M. W. Deem, *Phys. Rev. Lett.*, 1999, **83**, 1694.
55 H. Dominguez and M. Rivera, *Molec. Phys.*, 2002, **100**, 3829.
56 H. Dominguez and M. Rivera, *J. Chem. Phys.*, 2005, **123**, 066101.
57 M. A. Chavez-Tojo, R. Juarez-Maldonaldo and M. Medina-Noyola, *Phys. Rev. E.*, 2008, **77**, 040401(R).
58 M. Jardat, B. Hribar-Lee and V. Vlachy, *Phys. Chem. Chem. Phys.*, 2008, **10**, 449.
59 M. Jardat, B. Hribar-Lee and V. Vlachy, *to be submitted.*
60 J. J. Smith and I. Zarov, *Langmuir*, 2008, **24**, 2650.
61 B. Rotenberg, I. Pagonabarraga and D. D. Frenkel, *Faraday Discuss.*, 2010, **144**, 223.
62 S. F. Edwards and P. A. Anderson, *J. Phys. F: Metal. Phys.*, 1975, **5**, 965.
63 V. Dotsenko, *Introduction to the Replica Theory of Disordered Statistical Systems*, Cambridge University Press, Cambridge, 2001.
64 M. Mezard, G. Parisi and M. A. Virasoro, *Spin Glass Theory and Beyond*, World Scientific, Singapore, 1987.
65 J. A. Given, *J. Chem. Phys.*, 1992, **96**, 2287.
66 L. Sarkisov and P. A. Monson, *Phys. Rev. E*, 2000, **61**, 7231.
67 T. Ichiye and A. D. J. Haymet, *J. Chem. Phys.*, 1990, **93**, 8954.
68 D. M. Duh and A. D. J. Haymet, *J. Chem. Phys.*, 1992, **97**, 7716.
69 G. P. Morris and P. A. Monson, *Mol. Phys.*, 1983, **48**, 181.
70 J. C. Rasaiah, in *The Liquid State and its Electrical Properties (NATO ASI Series B, vol. 193)*, E. E. Kunhardt, L. G. Christophorou and L. H. Luessen, ed. Plenum Press, New York, 1989, pp. 89–142.
71 G. A. Mansoori, N. F. Carnahan, K. E. Starling and T. W. Leland, *J. Chem. Phys.*, 1971, **54**, 1523.
72 I. P. Yuhnovskii and M. F. Golovko, *Statisticheskaja teorija klassicheskih ravnovesnyh sistem*, Naukova dumka, Kiev, 1980, p. 134.
73 B. Hribar and V. Vlachy, *J. Phys. Chem. B*, 1997, **101**, 3457.
74 G. Pastore, H. Tatlipinar and M. P. Tosi, *Phys. Chem. Liq.*, 1996, **31**, 89.
75 M. Cardenas and M. P. Tosi, *J. Phys.: Condens. Matter*, 1997, **9**, 2767.
76 A. Trokhymchuk, G. A. Orozco, O. Pizio and V. Vlachy, *J. Colloid. Interface Sci.*, 1998, **207**, 379.
77 P. R. Van Tassel, *Phys. Rev. E*, 1999, **60**, R25.
78 G. Trefalt and B. Hribar-Lee, *Acta Chim. Slov.*, 2007, **54**, 503.
79 L. Zhang, S. Cheng and P. R. Van Tassel, *Phys. Rev. E*, 2001, **64**, 042101:1.
80 M. Lukšič, B. Hribar-Lee and V. Vlachy, *Acta Chim. Slov.*, 2007, **54**, 523.
81 M. Lukšič, V. Vlachy and O. Pizio, *Acta Chim. Slov.*, 2006, **53**, 292.
82 V. Vlachy, C. H. Marshall and A. D. J. Haymet, *J. Am. Chem. Soc.*, 1989, **111**, 4160.
83 V. Vlachy, *Langmuir*, 2001, **17**, 399.
84 F. H. J. Van der Heyden, D. Stein, K. Besternan, S. G. Lemay and C. Dekker, *Phys. Rev. Lett.*, 2006, **96**, 224502.
85 E. Lomba and J. J. Weis, *J. Chem. Phys.*, 2010, **132**, 104705:1.
86 L. Sarkisov and P. R. Van Tassel, *J. Phys.; Condens. Matter*, 2008, **20**, 333101.
87 D. Chandler and H. C. Andersen, *J. Chem. Phys.*, 1972, **57**, 1937.
88 F. Hirata, *Bull. Chem. Soc. Jpn.*, 1998, **71**, 1483.
89 C. C. Fleck and R. R. Netz, *Europhys. Lett.*, 2005, **70**, 341.
90 R. Podgornik and A. Naji, *Europhys. Lett.*, 2006, **74**, 712.
91 A. Naji and R. Podgornik, *Phys. Rev. E*, 2005, **72**, 041402.
92 Y. S. Mamasakhlisov, A. Naji and R. Podgornik, *J. Stat. Phys.*, 2008, **133**, 659.
93 P. Bryk, A. Patrykiejew, J. Reszko-Zygmunt and S. Sokołowski, *Mol. Phys.*, 1999, **96**, 1509.
94 D. Boda, D. Henderson, R. Rowley and S. Sokołowski, *J. Chem. Phys.*, 1999, **111**, 9382.
95 M. Schmidt, *J. Phys.:Condens. Matter*, 2005, **17**, S3481.
96 M. Schmidt, *Phys. Rev. E*, 2002, **66**, 041108.
97 L. Ibarra Bracamontes, O. Pizio, S. Sokołowski and A. Trokhymchuk, *Mol. Phys.*, 1999, **96**, 1341.
98 O. Pizio and S. Sokołowski, *Phys. Rev. E*, 1997, **56**, R63.
99 A. Kovalenko, S. Sokołowski, D. Henderson and O. Pizio, *Phys. Rev. E*, 1998, **57**, 1824.
100 G. E. Kapellos, T. S. Alexiou and A. C. Payatakes, *Mathematical Biosciences*, 2010, **225**, 83.
101 I. Pagonabarraga, B. Rotenberg and D. Frenkel, *Phys. Chem. Chem. Phys.*, 2010, **12**, 9566.
102 T. Lemaire, J. Kaiser, S. Naili and S. V, *Mech. Res. Comm.*, 2010, **37**, 495.
103 J. Kaiser, T. Lemaire, S. Naili and V. Sansalone, *Comptes Rendus Mechanique*, 2009, **337**, 768.

104 V. Marry, J. F. Dufreche, M. Jardat, G. Meriguet, P. Turq and F. Grun, *Colloids and Surfaces A: Physicochem. Eng. Aspects*, 2003, **222**, 147.
105 B. Rotenberg, J.-F. Dufreche, B. Bagchi, E. Giffaut, J.-P. Hansen and P. Turq, *J. Chem. Phys.*, 2006, **124**, 154701:1.
106 B. Rotenberg, V. Marry, R. Vuilleumier, N. Malikova, C. Simon and P. Turq, *Geochim. Cosmochim. Acta*, 2007, **71**, 5089.
107 B. Rotenberg, J.-P. Morel, V. Marry, P. Turq and Morel-Desrosiers, *Geochim. Cosmochim. Acta*, 2009, **73**, 4034.
108 M. Jardat, J.-F. Dufreche, V. Marry, B. Rotenberg and P. Turq, *Phys. Chem. Chem. Phys.*, 2009, **11**, 2023.
109 C. B. Roland, K. A. Hatch, M. Prentiss and E. I. Shakhnovich, *Phys. Rev. E.*, 2009, **79**, 051923.
110 M. Holovko and W. Dong, *J. Phys. Chem. B*, 2009, **113**, 6360.